

THE ABILITY OF ALLICIN TO CROSS BLOOD-BRAIN BARRIER AND  
ITS EFFECTS ON PATHOGENS CAUSING MENINGITIS



A Thesis Submitted in Partial Fulfillment of the Requirements for the  
Degree of Master of Science in Microbiology  
Suranaree University of Technology  
Academic Year 2021

ความสามารถของอัลลีลซิงในการผ่านแนวกั้นระหว่างหลอดเลือดกับสมอง  
และผลต่อเชื้อก่อโรคเยื่อหุ้มสมองอักเสบ



นางสาวกัญท์กวี ศาสตร์สันติธรรม

วิทยานิพนธ์นี้เป็นส่วนหนึ่งของการศึกษาตามหลักสูตรปริญญาวิทยาศาสตรมหาบัณฑิต  
สาขาวิชาจุลชีววิทยา  
มหาวิทยาลัยเทคโนโลยีสุรนารี  
ปีการศึกษา 2564

THE ABILITY OF ALLICIN TO CROSS BLOOD-BRAIN BARRIER AND  
ITS EFFECTS ON PATHOGENS CAUSING MENINGITIS

Suranaree University of Technology has approved this thesis submitted in partial fulfillment of the requirements for a Master's Degree.

Thesis Examining Committee



(Dr. Nisa Patikarnmonthon)

Chairperson



(Asst. Prof. Dr. Oratai Weeranantapan)

Member (Thesis Advisor)



(Assoc. Prof. Dr. Nuanoi Chudapongse)

Member (Thesis Co-advisor)



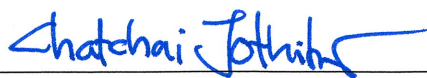
(Asst. Prof. Dr. Piyada Ngersoungnern)

Member



(Dr. Pishyaporn Sritangos)

Member



(Assoc. Prof. Dr. Chatchai Jothiyangkoon)

Vice Rector for Academic Affairs  
and Quality Assurance



(Prof. Dr. Santi Maensiri)

Dean of Institute of Science

กัณฑ์กวี ศาสน์สันติธรรม : ความสามารถของอัลลิซินในการผ่านแนวกันระหว่างหลอดเลือด  
กับสมองและผลต่อเชื้อก่อโรคเยื่อหุ้มสมองอักเสบ (THE ABILITY OF ALLICIN TO CROSS  
BLOOD-BRAIN BARRIER AND ITS EFFECTS ON PATHOGENS CAUSING MENINGITIS)  
อาจารย์ที่ปรึกษา : ผู้ช่วยศาสตราจารย์ ดร.อรัญญ์ วีระนนทนาพันธ์, 61 หน้า.

คำสำคัญ: แนวกันระหว่างหลอดเลือดกับสมอง/ อัลลิซิน/ โรคเยื่อหุ้มสมองอักเสบ

โรคเยื่อหุ้มสมองอักเสบเป็นโรคที่มีความอันตรายถึงแก่ชีวิต ซึ่งจะเกิดขึ้นเมื่อเชื้อโรคสามารถผ่านแนวกันระหว่างหลอดเลือดกับสมองเข้ามาได้และส่งผลให้เกิดการอักเสบที่บริเวณเยื่อหุ้มสมอง สารอัลลิซิน ซึ่งเป็นสารออกฤทธิ์สำคัญที่พบเป็นหลักในกระเทียมนั้น มีฤทธิ์ต้านเชื้อแบคทีเรียหลายชนิด รวมถึงเชื้อก่อโรคเยื่อหุ้มสมองอักเสบบางชนิด ในการศึกษาเบื้องต้นได้มีการรายงานถึงความเป็นไปได้ที่อัลลิซินจะมีความสามารถในการผ่านแนวกันระหว่างหลอดเลือดกับสมอง อย่างไรก็ตาม ยังไม่มีหลักฐานใดที่สามารถพิสูจน์ได้โดยตรง ดังนั้น วัตถุประสงค์ของงานวิจัยนี้จึงต้องการศึกษาความสามารถของอัลลิซินในการผ่านแนวกันระหว่างหลอดเลือดกับสมองและผลต่อเชื้อก่อโรคเยื่อหุ้มสมองอักเสบ จากการศึกษาฤทธิ์ต้านเชื้อแบคทีเรียของอัลลิซินโดยวิธี broth microdilution พบว่าค่าความเข้มข้นที่ต่ำสุดที่สามารถยับยั้งเชื้อได้ของอัลลิซินต่อเชื้อแบคทีเรียชนิด *N. meningitidis* ATCC13090 DMST7950, *L. monocytogenes* DMST20093, *E. coli* TISTR780, *E. coli* O157:H7 DMST12743, และ MRSA DMST20654 คือ 3, 30, 25, 25, และ 15 ไมโครกรัมต่อมิลลิลิตร ตามลำดับ ค่าความเข้มข้นของอัลลิซินซึ่งไม่เป็นพิษต่อเซลล์ hCMEC/D3 นั้นสามารถระบุได้โดยวิธีการทดสอบกับสาร MTT จากนั้น ความเข้มข้นของอัลลิซินที่ไม่เป็นพิษต่อเซลล์ซึ่งได้แก่ 0.5, 1, 2 และ 5 ไมโครกรัมต่อมิลลิลิตรจึงถูกนำไปใช้ในการทดสอบความสามารถของอัลลิซินในการผ่านแบบจำลองของแนวกันระหว่างหลอดเลือดกับสมอง และเทคนิค high-performance liquid chromatography (HPLC) ถูกนำมาใช้เพื่อวิเคราะห์ค่าความเข้มข้นของอัลลิซินที่สามารถผ่านแบบจำลองของแนวกันระหว่างหลอดเลือดกับสมอง โดยผลการทดสอบพบว่า ไม่สามารถตรวจพบสารอัลลิซินได้ทั้งในส่วนประกอบด้านบนและด้านล่างของแบบจำลอง ในทางตรงกันข้าม สารอัลลิซินนั้นยังคงตรวจพบได้ในแบบจำลองที่ปราศจากเซลล์ทั้งแบบที่มีการเคลือบและไม่เคลือบคอลลาเจน จากผลการทดลองนี้แสดงให้เห็นว่า สารอัลลิซินไม่ได้หายไปเนื่องจากติดอยู่ในคอลลาเจนหรือแผ่นเมมเบรนของแบบจำลอง การทดสอบความสามารถในการดูดซึมของเซลล์โดยอ้อมได้ถูกดำเนินการต่อไปและผลการทดลองชี้แนะว่า เซลล์ hCMEC/D3 ได้มีการดูดซึมอัลลิซินเข้าสู่เซลล์ การค้นพบจากการศึกษานี้ นำไปสู่การตั้งข้อสันนิษฐานใหม่ที่ว่า สารอัลลิซินที่ใช้ในการทดสอบนั้นได้ถูกดูดซึมเข้าสู่เซลล์ hCMEC/D3 จึงส่งผลให้ไม่สามารถตรวจสอบปริมาณสารอัลลิซินที่สามารถผ่านแบบจำลองของ

แนวกั้นระหว่างหลอดเลือดกับสมองได้ อย่างไรก็ตาม ผลการศึกษานี้เผยให้เห็นว่าเซลล์ hCMEC/D3 สามารถดูดซึมสารอัลลิซินความเข้มข้น 5 ไมโครกรัมต่อมิลลิเมตรเข้าสู่เซลล์ได้ ซึ่งเป็นปริมาณที่อาจจะเพียงพอที่จะผ่านแนวกั้นระหว่างหลอดเลือดกับสมองและส่งผลยับยั้งการเจริญของเชื้อก่อโรคเยื่อหุ้มสมองอักเสบชนิด *N. meningitidis* ได้



สาขาวิชาปรีคลินิก  
ปีการศึกษา 2564

ลายมือชื่อนักศึกษา Kankawi Satsantitham

ลายมือชื่ออาจารย์ที่ปรึกษา Oratai Weerananantapan

ลายมือชื่ออาจารย์ที่ปรึกษาร่วม ร.ร.

ลายมือชื่ออาจารย์ที่ปรึกษาร่วม ร.ร.

KANKAWI SATSANTITHAM : THE ABILITY OF ALLICIN TO CROSS BLOOD-BRAIN BARRIER AND ITS EFFECTS ON PATHOGENS CAUSING MENINGITIS.  
THESIS ADVISOR : ASST. PROF. ORATAI WEERANANTANAPAN, Ph.D. 61 PP.

Keyword: BLOOD-BRAIN BARRIER/ ALLICIN/ MENINGITIS

Meningitis is a life-threatening disease that occurs when the pathogens can penetrate the blood-brain barrier (BBB) and cause inflammation of the meninges. Allicin, a major active compound derived from garlic, exhibits antibacterial activity against a wide range of bacteria, including some of the meningitis pathogens. There are studies suggesting that allicin may be able to pass the BBB; however, the direct evidence to prove that has not been reported yet. The aims of this study were to investigate the capability of allicin to pass BBB and its antibacterial activity against pathogens causing meningitis. The broth microdilution method was used to investigate the antibacterial activity of allicin against tested bacterial pathogens. The results revealed that the minimum inhibitory concentration (MIC) values of allicin against *N. meningitidis* ATCC13090 DMST7950, *L. monocytogenes* DMST20093, *E. coli* TISTR780, *E. coli* O157:H7 DMST12743, and MRSA DMST20654 were 3, 30, 25, 25, and 15 µg/ml, respectively. The non-toxicity concentrations of allicin on hCMEC/D3 cells were determined by using the MTT assay. Then, the non-toxicity concentrations of allicin, which are 0.5, 1, 2, and 5 µg/ml, were used to investigate the ability of allicin to cross the *in vitro* BBB model. The high-performance liquid chromatography (HPLC) analysis was used to determine the allicin concentration that was able to pass the *in vitro* BBB model. The results showed that allicin could not be detected on both apical (AP) and basolateral (BL) chambers of the *in vitro* BBB model. On the other hand, allicin was still detected in collagen-coated and non-collagen-coated control inserts (cell-free). These results indicated that allicin was not trapped in the collagen or membrane of the insert. The indirect cellular uptake experiments were performed and the results suggested that allicin was absorbed by hCMEC/D3 cells. These findings led to the new presumption that allicin could be uptaken into hCMEC/D3 cells resulting in an undetectable concentration of allicin that passes through the *in vitro* BBB model.

However, the results in this study revealed that hCMEC/D3 cells uptake allicin 5  $\mu\text{g}/\text{ml}$  into the cells, suggesting that allicin may have the potential to pass the BBB with a sufficient dose to inhibit the meningitis pathogen *N. meningitidis*.



School of Preclinical Sciences  
Academic Year 2021

Student's Signature Kankami Satsantitkam

Advisor's Signature Oratai Weerananantapanom

Co-advisor's Signature 268

Co-advisor's Signature MH

## ACKNOWLEDGEMENTS

I would like to express my deepest appreciation to my thesis advisor, Asst. Prof. Dr. Oratai Weeranantanapan. The completion of this thesis could not have been possible without her superb guidance, encouragement, care, and support. I am delighted to have been under her supervision throughout my time as a master's student. I also extend my gratitude to Assoc. Prof. Dr. Nuannoi Chudapongse and Asst. Prof. Nawarat Nantapong for their valuable advice and suggestions as my thesis co-advisors.

I would like to sincerely thank my chairperson of the thesis examining committee, Dr. Nisa Patikarnmonthon, and the committee members, Asst. Prof. Dr. Piyada Ngernsounghern and Dr. Pishyaporn Sritangos, for their excellent suggestions regarding this thesis.

I would like to thank the One Research One Grant (OROG) scholarship from the Suranaree University of Technology for assistance in research finance support. I am also grateful to all the staff at the Suranaree University of Technology for their kindness and assistance throughout the period of this research. Thanks to my laboratory colleagues and friends for always supporting and willing to help in every circumstance.

I wish to express my final acknowledgment to my family, who always be by my side. Without their understanding, love, and support, I would not be here.

Kankawi Satsantitham

# CONTENTS

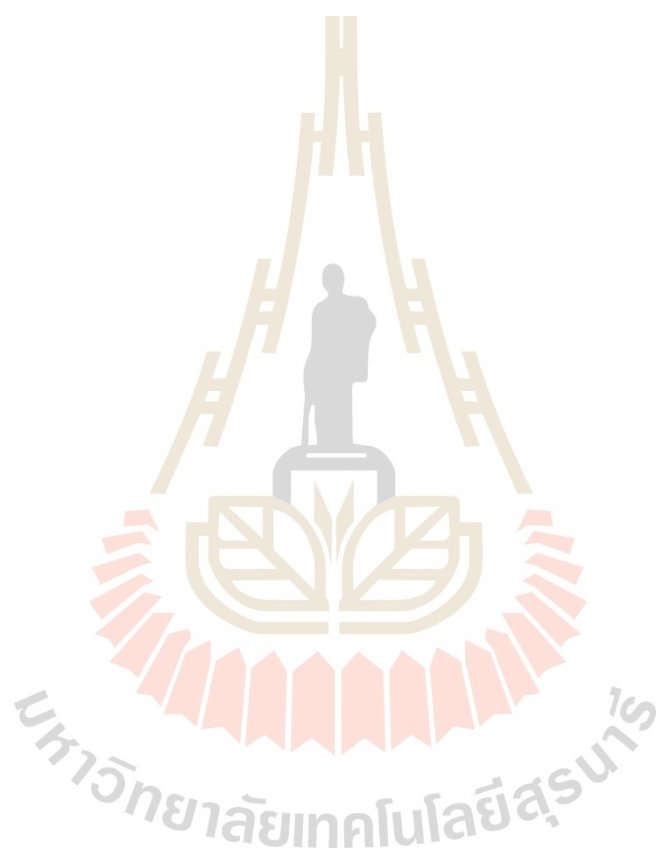
	Page
ABSTRACT IN THAI.....	I
ABSTRACT IN ENGLISH.....	II
ACKNOWLEDGEMENTS .....	V
CONTENTS.....	VI
LIST OF TABLES.....	IX
LIST OF FIGURES .....	X
LIST OF ABBREVIATIONS .....	XI
<b>CHAPTER</b>	
<b>I INTRODUCTION.....</b>	<b>1</b>
1.1 Background / Problem.....	1
1.2 Research objectives.....	2
1.3 Research hypothesis .....	2
1.4 Scope and limitations of the study .....	2
<b>II LITERATURE REVIEW.....</b>	<b>4</b>
2.1 Blood-brain barrier (BBB).....	4
2.2 The BBB models.....	6
2.2.1 <i>In vivo</i> BBB models.....	6
2.2.2 <i>In vitro</i> BBB models.....	7
2.2.2.1 The cell types used in <i>in vitro</i> BBB models .....	7
2.2.2.2 Static <i>in vitro</i> BBB models (Transwell BBB models).....	8
2.2.2.2 Microfluidic <i>in vitro</i> BBB models (BBB-on-a-chip).....	10
2.3 Brain infectious diseases .....	12
2.4 Allicin.....	16
2.4.1 Antibacterial properties of allicin .....	18
2.4.2 Mechanism of action of allicin on bacteria.....	18

## CONTENTS (Continued)

	Page
2.5 The possibility of allicin to cross the BBB .....	19
<b>III MATERIALS AND METHODS .....</b>	<b>20</b>
3.1 Materials.....	20
3.1.1 Bacterial strains and cell lines.....	20
3.1.2 Media and reagents .....	20
3.2 Methods.....	22
3.2.1 Minimum inhibitory concentration (MIC) assay.....	22
3.2.2 Cell viability assay.....	22
3.2.3 The construction of the <i>in vitro</i> BBB model .....	23
3.2.3.1 Trans-endothelial electrical resistance measurement (TEERs) .....	24
3.2.3.2 Lucifer yellow permeability assay .....	24
3.2.4 Determination of allicin in the <i>in vitro</i> BBB model by HPLC analysis.....	25
3.2.5 Cellular uptake experiments .....	26
3.2.6 Statistical analysis .....	26
<b>IV RESULTS AND DISCUSSION.....</b>	<b>27</b>
4.1 Minimum inhibitory concentration (MIC) values of allicin against bacterial pathogens .....	27
4.2 The cytotoxicity of allicin on hCMEC/D3 cells .....	29
4.3 The ability of allicin to cross the <i>in vitro</i> BBB model .....	30
4.4 The uptake of allicin by hCMEC/D3 cells .....	37
<b>V CONCLUSION .....</b>	<b>43</b>
REFERENCES .....	44
APPENDICES.....	56
APPENDIX A LABORATORY EQUIPMENT.....	57

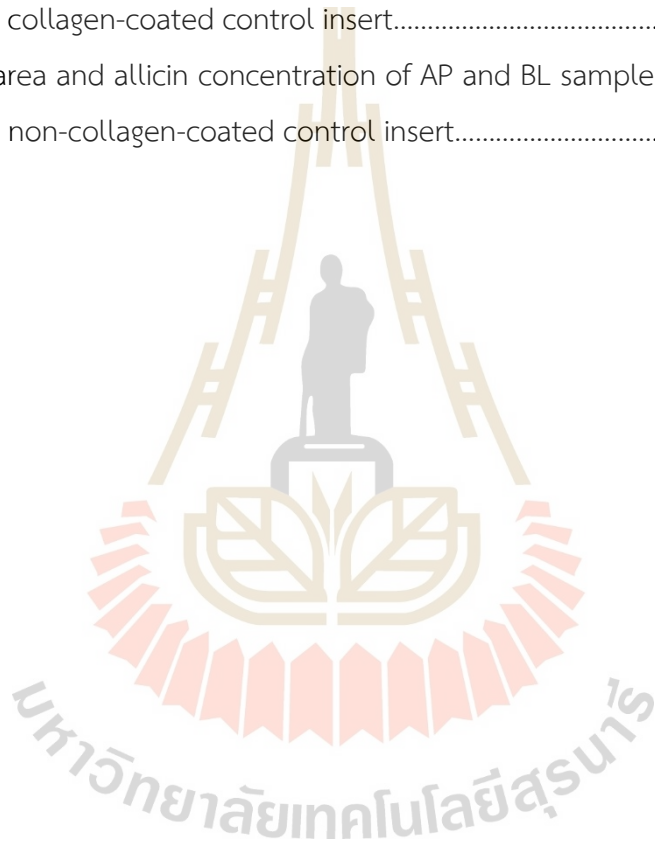
## CONTENTS (Continued)

	Page
APPENDIX B STANDARD CURVE OF ALLICIN.....	59
APPENDIX C TEMPERATURE TEST OF ALLICIN.....	60
CURRICULUM VITAE.....	61



## LIST OF TABLES

Table	Page
4.1 The MIC values of allicin against bacterial pathogens.....	27
4.2 Peak area and allicin concentration of AP and BL samples of the collagen-coated control insert.....	34
4.3 Peak area and allicin concentration of AP and BL samples of the non-collagen-coated control insert.....	35



## LIST OF FIGURES

Figure	Page
2.1	The blood-brain barrier structure.....4
2.2	Transport mechanisms across the blood-brain barrier.....5
2.3	Schematic representation of monoculture and co-culture <i>in vitro</i> BBB models.....10
2.4	Schematic representation of microfluidic <i>in vitro</i> BBB model or BBB-on-a-chip.....11
2.5	Pathogenesis of bacterial meningitis development.....14
2.6	Mechanisms involved in the pathogen penetrate across the blood-brain barrier.....15
2.7	Enzyme-catalyzed biosynthesis of allicin.....16
3.1	The <i>in vitro</i> BBB model.....24
4.1	The cytotoxicity of allicin on hCMEC/D3 cells.....29
4.2	HPLC analysis of HBSS (baseline) and standard allicin.....32
4.3	HPLC analysis of allicin samples from the <i>in vitro</i> BBB model.....33
4.4	HPLC analysis of allicin samples from the collagen-coated control insert (cell-free) tested with allicin 5 µg/ml.....34
4.5	HPLC analysis of allicin samples from the non-collagen-coated control insert (cell-free) tested with allicin 5 µg/ml.....35
4.6	The schematic represents 3 possibilities movement of allicin across the <i>in vitro</i> BBB model after 3 h of treatment.....37
4.7	The cellular uptake of allicin by hCMEC/D3 cells.....39
4.8	The cellular uptake of allicin (5 µg/ml) by hCMEC/D3 cells.....40

## LIST OF ABBREVIATIONS

ATCC	American Type Culture Collection
BBB	Blood-brain barrier
CECs	Cerebral microvessel endothelial cells
CFU	Colony forming unit
cm	Centimeter
CNS	Central nervous system
CO <sub>2</sub>	Carbon dioxide
CSF	Cerebrospinal fluid
°C	Degree Celsius
DMSO	Dimethyl sulfoxide
DMST	Department of Medical Sciences Thailand
DPBS	Dulbecco's phosphate-buffered saline
g	Gram
g/l	Gram per liter
GSH	Glutathione
GSSA	S-allylmercaptoglutathione
h	Hour
HBSS	Hank's Balanced Salt Solution
HPLC	High performance liquid chromatography
hTERT	Human telomerase reverse transcriptase
iPSCs	Induced pluripotent stem cells
IRBI	Ischemia-reperfusion brain injury
LY	Lucifer yellow
mAU	Milli-Absorbance Units
mg/ml	Milligram per milliliter
min	Minute
ml	Milliliter

**LIST OF ABBREVIATIONS (Continued)**

mm	Millimeter
MMPs	Matrix metalloproteinases
MRI	Magnetic resonance imaging
MTT	3-(4,5-dimethylthiazol-2-yl)-2,5-diphenyltetrazolium bromide
OD	Optical density
PBS	Phosphate buffered saline
PET	Positron emission tomography
P-gp	P-glycoprotein
ROS	Reactive oxygen species
SARS-CoV-2	Severe Acute Respiratory Syndrome Coronavirus 2
sec	Second
SPECT	Single-photon emission computed tomography
TEER	Trans-endothelial electrical resistance
TISTR	Thailand Institute of Scientific and Technological Research
TJs	Tight junctions
ZO-1	Zonula occludens-1
µg/ml	Microgram per milliliter
µl	Microliter

# CHAPTER I

## INTRODUCTION

### 1.1 Background / Problem

The homeostasis of the central nervous system (CNS) is maintained by the blood-brain barrier (BBB), which comprises of various types of cells such as pericytes, astrocytes, and endothelial cells that contain the tight junctions to connect between the cells and allow a highly regulated BBB permeability. The BBB strictly controls the passage of any substances that can be transferred from the circulation into the brain. It also acts as a protective barrier that shields the CNS from toxins and pathogens circulating in the blood (Abbott et al., 2010). However, certain bacteria possess the ability to penetrate the BBB to cause meningitis, which is a serious and life-threatening disease (Doran et al., 2016).

The BBB models have been used to develop the treatment for brain disorders. Among the various types of BBB models that were established to study the drug delivery to CNS, the transwell BBB models are the simplest *in vitro* BBB model that provides easy handling and cost-effectiveness (Jackson et al., 2019). The human cerebral microvascular endothelial cell line hCMEC/D3 is well-characterized and the most widely used for constructing the *in vitro* BBB models. The hCMEC/D3 cells represent a stable and easily grown BBB model, which appears to be suitable for drug uptake studies (Weksler et al., 2013).

Allicin is a principal active compound of freshly crushed garlic (*Allium sativum*). Previous studies have revealed that allicin possesses a wide range of biological properties, which are anti-inflammatory (Alam et al., 2018), antihypertensive (Borlinghaus et al., 2014), anticancer (Oommen et al., 2004), and antimicrobial activities (Ankri and Mirelman, 1999). Recently, Itepu et al. (2019) have constructed the 2D structure of allicin and its modified molecule to examine their ability to penetrate BBB by using the SwissADME server. The study showed that the calculated polar surface

area (PSA) of allicin is 61.58 angstroms, which is predicted to be able to pass BBB because the previous study has showed that the molecules that have the PSA less than 90 angstroms can penetrate the BBB (Hitchcock and Pennington, 2006). Moreover, the neuroprotective effects on ischemia-reperfusion brain injury (IRBI) in mice has been reported, leading to the presumption that allicin may be able to pass BBB (Kong et al., 2017). However, there is no direct evidence clearly demonstrating that allicin can pass BBB. According to a broad spectrum of antibacterial activity of allicin against Gram-positive and Gram-negative bacteria (Ankri and Mirelman, 1999), the aims of this research are to investigate the capability of allicin to pass BBB and its antibacterial activity against pathogens causing meningitis.

## 1.2 Research objectives

- 1.2.1 To examine the antibacterial activity of allicin on pathogens causing meningitis.
- 1.2.2 To investigate the cytotoxicity of allicin on hCMEC/D3 cells.
- 1.2.3 To investigate the ability of allicin to pass the blood-brain barrier *in vitro* model.
- 1.2.4 To investigate the uptake of allicin by hCMEC/D3 cells.

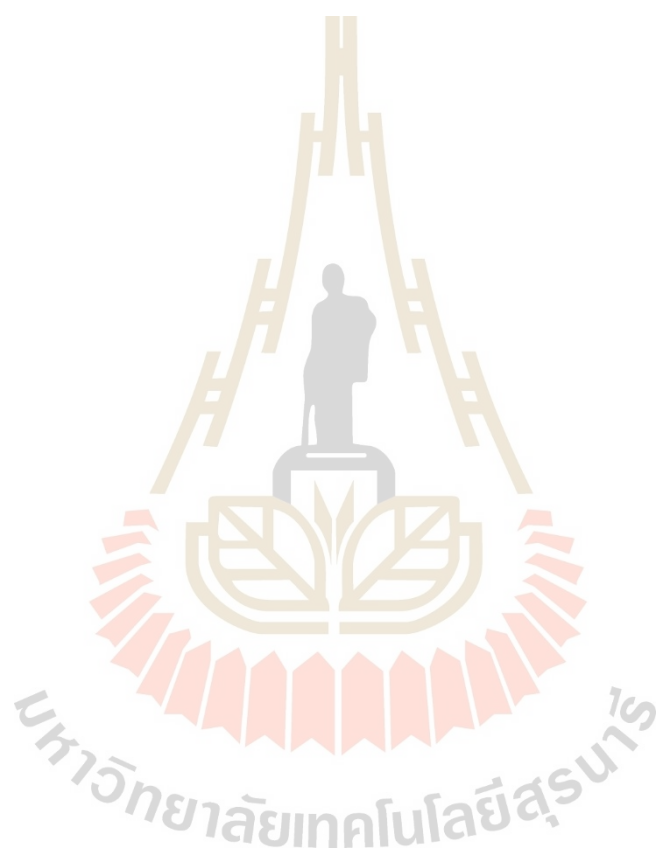
## 1.3 Research hypothesis

Allicin passes the blood-brain barrier *in vitro* model and inhibits the bacterial pathogens causing meningitis.

## 1.4 Scope and limitations of the study

In this study, the antibacterial activity of allicin against bacterial pathogens and the cytotoxicity of allicin on hCMEC/D3 cells were evaluated. The *in vitro* BBB model was used to observe the ability of allicin to pass the BBB. The uptake of allicin into hCMEC/D3 cells was investigated indirectly by cellular uptake experiments. The limitation of this study was the obtained results could not completely prove that allicin

has the ability to cross the *in vitro* BBB model. Further study of the ability of allicin to cross the *in vitro* BBB model with extended duration of experiments, the direct allicin uptake experiments, and the direct experiments of allicin formation change within the hCMEC/D3 cells are required in future studies.



## CHAPTER II

### LITERATURE REVIEW

#### 2.1 Blood-brain barrier (BBB)

The brain of all organisms with a well-developed central nervous system (CNS) has a blood-brain barrier (BBB) (Abbott, 2005). The BBB consists of the capillary basement membrane and various types of cells such as endothelial cells, pericytes that embrace the endothelium, and astrocytes end-feet which connect to both the endothelium and pericytes (Figure 2.1). All the BBB components are believed to be essential for the normal function and stability of the BBB (Ballabh et al., 2004).

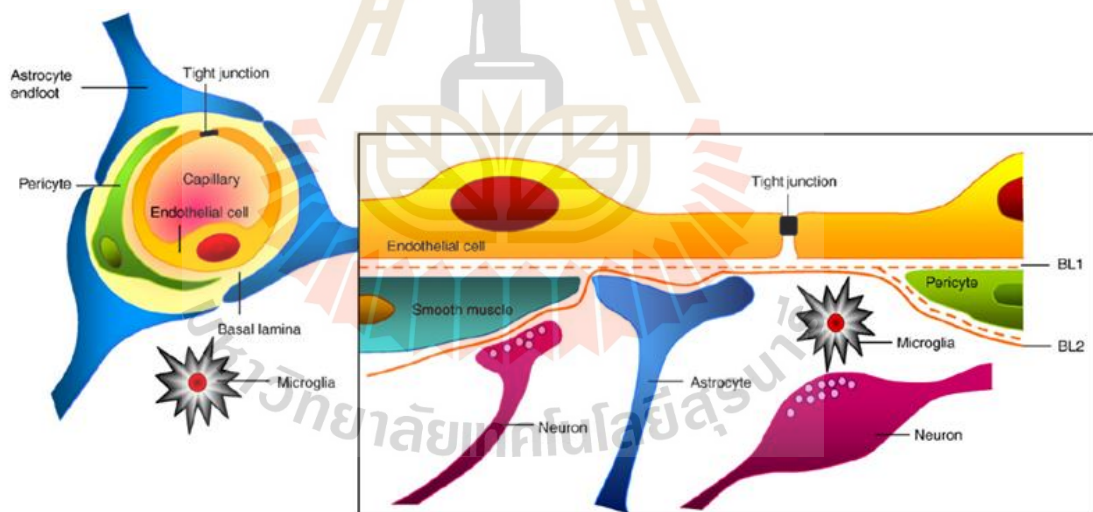


Figure 2.1 The blood-brain barrier structure (Abbott et al., 2010).

Brain endothelial cells are connected to each other with tight junctions (TJs) which allow a highly regulated BBB permeability (Jackson et al., 2019). BBB plays a major role in controlling the passage of any substances that can be transferred from the blood into the brain. The circulating molecules can selectively pass into the brain

through several transport mechanisms (Figure 2.2). The paracellular transport of water-soluble (hydrophilic) molecules is restricted to moving across the BBB by TJs, whereas the small lipid-soluble (lipophilic) molecules such as  $O_2$  and  $CO_2$  can diffuse across the plasma membrane of BBB along their concentration gradients via the transcellular lipophilic pathway (Grieb et al., 1985). The necessary nutrients such as glucose, amino acids, and nucleosides can be selectively transported through the brain via transporter proteins (Barar et al., 2016). The larger molecules that are able to attach to the cell-surface receptors, such as insulin, leptin, and iron transferrin, could be uptaken via receptor-mediated endocytosis (Pardridge et al., 1985; Zhang and Pardridge, 2001). The substance with cationized ligands or peptides such as albumin induces absorptive transcytosis (Lu et al., 2014). On the contrary, the neurotoxic substances and pathogens are restricted to enter the brain (Daneman and Prat, 2015). Thus, the BBB can provide a stable fluid microenvironment (homeostasis), which is essential for neural function and protect the CNS tissue from possible damages (Abbott et al., 2010). The highly selective permeability of the BBB also provides an obstacle for drug delivery to the CNS. Therefore, major efforts have been made to generate methods to deliver drugs through the BBB (Larsen et al., 2014).

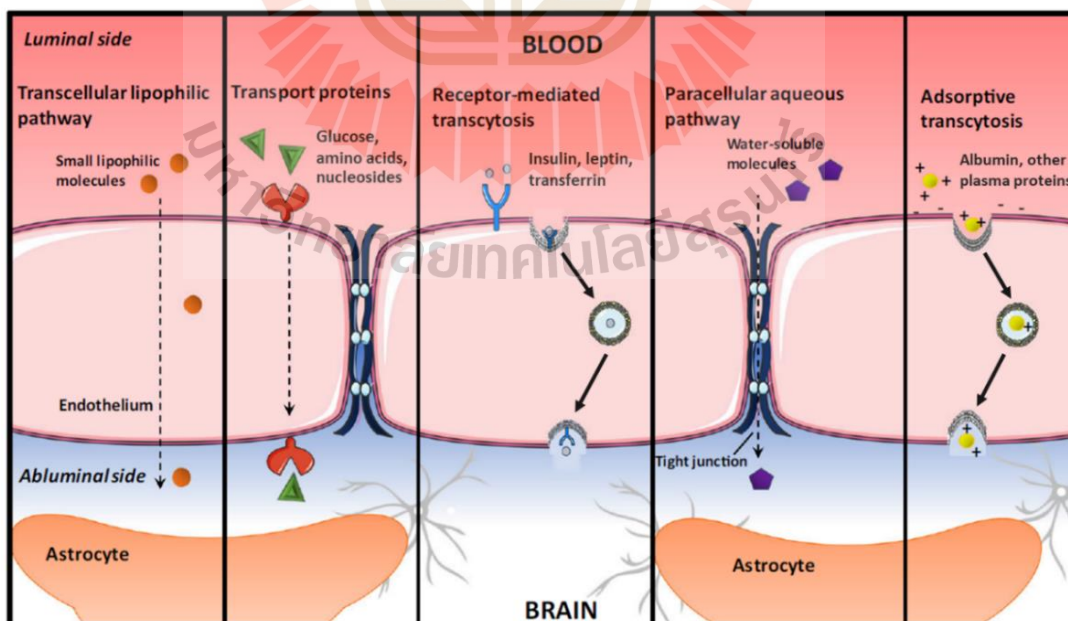


Figure 2.2 Transport mechanisms across the blood-brain barrier (modified from Jena et al., 2020)

## 2.2 The BBB models

In order to study and develop the treatment of CNS-related disorders, several types of the BBB model, *in vivo* and *in vitro*, are utilized to investigate the drug delivery across the BBB.

### 2.2.1 *In vivo* BBB models

The utilization of living animals as the BBB models or *in vivo* BBB models allows the prediction of therapeutic candidates delivered to CNS because they replicate the complexity of structural, physiological, and functional of the BBB in its natural habit (Passeleu-Le Bourdonnec et al., 2013). The rodent models (mice and rats) are the widely used mammalian models due to rodents and humans shared similar brain features in morphology, physiology, and pathology (Sharma et al., 2019). In order to assess the study of drug transport through the BBB of rodent models, several techniques both noninvasive and invasive could be performed. The noninvasive techniques, which are live-imaging (e.g., magnetic resonance imaging (MRI), positron emission tomography (PET), and single-photon emission computed tomography (SPECT)), can be used to study BBB integrity, permeability, brain uptake kinetics, and the function of efflux transporters in the alive animals (Pandey et al., 2015). On the other hand, most invasive techniques require animal sacrifice to determine the concentration of the test compounds within the brain, such as brain uptake index (BUI) techniques, brain efflux index techniques, quantitative autoradiography, and *in situ* brain perfusion method (Bicker et al., 2014). Although rodent models are useful for pre-clinical trials, performing high-throughput studies could be difficult and very expensive (Jackson et al., 2019).

Recently, another *in vivo* BBB model that has been introduced is zebrafish (*Danio rerio*). This organism possesses a small size and easy cultivation, which suitable for high-throughput studies with cost and time effective (Jackson et al., 2019). The BBB of zebrafish has a similar structure and function to higher vertebrates, such as mice and rats (Sharma et al., 2019). Moreover, the BBB in adult zebrafish has been found to express the TJs proteins (e.g., claudin-5 and zonula occludens-1 (ZO-1)) and efflux transporter P-glycoprotein (P-gp) which is homolog to the human BBB (Jeong et al.,

2008; Umans and Taylor, 2012). Although the transporters of BBB need more well-characterization, the zebrafish has proved to be a reliable BBB model for drug delivery studies (Jackson et al., 2019; Sharma et al., 2019). However, the utilization of *in vivo* models requires expertise in animal handling and consideration of ethical concerns. Furthermore, it has been revealed that >80% of drug candidates can be successfully used in animals but failed in humans due to the difference in species (Chin and Goh, 2018).

## 2.2.2 *In vitro* BBB models

### 2.2.2.1 The cell types used in *In vitro* BBB models

The *in vitro* BBB models could be constructed by using primary and immortalized cell lines derived from various sources, such as bovine, porcine, mouse, rat, and human. The primary brain endothelial cells can be harvested from brain tissue isolation. This cell type provides a close relevance phenotypic of the *in vivo* BBB. However, the difficulty in the isolation and purification processes results in time-consuming, labor-intensive, and receiving a very low yield. The limitations of primary brain endothelial cells also include the ethical issue and the rapid loss of BBB properties through the culture period; thus, the sub-culture and storage for future use are impossible (Passeleu-Le Bourdonnec et al., 2013; Bicker et al., 2014). Therefore, several immortalized brain endothelial cell lines from a variety of species, such as rodents (RBE4, b.End3, b.End5), porcine (PBMEC/C1-2), bovine (t-BBEC-117), and humans (HBMEC, hCMEC/D3) were created to overcome the limitations of primary cells (Sobue et al., 199; Neuhaus et al., 2006; Sivandzade and Luca Cucullo, 2018).

The hCMEC/D3 or immortalized human cerebral microvascular endothelial cell line is widely used and well-characterized. It was produced from cerebral microvessel endothelial cells (CECs) of dead epilepsy patients by transduction with lentiviral vectors carrying the SV40 T antigen and human telomerase reverse transcriptase (hTERT) (Weksler et al., 2005). According to this immortalization process, hCMEC/D3 cells are able to give a large yield and generate at least 35 passages while remaining the same traits of the human BBB genotype and phenotype (Weksler et al., 2013). The hCMEC/D3 cells might form low tightness monolayers due to the low

expression of some enzymes and transporters. However, the barrier function was considered adequate (Daniels et al., 2013). The hCMEC/D3 cells possess the major advantage in providing a stable and easily grown BBB model. It is suitable to study the drug uptake and investigate the response of brain endothelial cells to human pathogens and inflammatory stimuli (Weksler et al., 2013).

The construction of the *in vitro* BBB model with brain endothelial cell-like cells derived from human induced pluripotent stem cells (iPSCs) is recently growing attention for BBB modeling. The previous studies revealed that iPSC-derived brain endothelial cells expressed the TJs protein, nutrient transporters, and efflux transporters, which could lead to the effective exhibition of the barrier function (Lippmann et al., 2013). However, further characterization of iPSC-derived brain endothelial cells is required for standard use. In order to mimic the rearrangement of BBB *in situ* and increase the tightness of *in vitro* BBB models, other neurovascular unit cells, such as astrocytes, pericytes, and neurons, could be used in co-culture BBB models (Jackson et al., 2019).

#### **2.2.2.2 Static *In vitro* BBB models (Transwell BBB models)**

The static *in vitro* BBB models or transwell BBB models have been established to study the physiology and pathology of the BBB, which would lead to the development of drug delivery to the CNS with more versatility and lower cost compared to the *in vivo* models (Jackson et al., 2019). The commonly used static *in vitro* BBB models divided into monoculture and co-culture models (Figure 2.3). Monoculture is the simplest BBB model in which only brain microvascular endothelial cells (BMECs) are grown on the microporous membrane (0.2-0.4  $\mu\text{m}$ ) of the transwell insert system. The upper chamber of the insert mimics the blood side, whereas the lower chamber mimics the brain side (Pardridge et al., 1990). Co-culture models are further divided into (1) Non-contact co-culture: BMECs are seeded on the upper surface of the insert membrane, while the astrocytes (or pericytes) are seeded at the bottom of the lower chamber to act as the “feeder cells” for endothelium induction (Cecchelli et al., 1999); (2) Contact co-culture: BMECs are seeded on the upper surface of the insert membrane with astrocytes on the lower surface. This model allows direct

contact between two CNS cell types (Dehouck et al., 1990); and (3) Triple culture: BMECs are seeded on the upper surface of the insert membrane, pericytes on the lower surface, and astrocytes at the bottom of the lower chamber. This model allows the interactions between three CNS cell types and mimics the cell arrangement within the neurovascular unit (Nakagawa et al., 2009). The monoculture model is more simple and easier to handle compared to the co-culture models. However, the co-culture models allow the interaction between BMECs and other CNS cell types which promotes BBB regulation and would be more closely mimic to the BBB *in vivo*. Although the co-culture models are more reliable *in vitro* BBB models but the involvement of the different cell types in the same model also leads to a more demanding workload and experimental skills (Helms et al., 2016; Bagchi et al., 2019). The integrity and permeability of TJs forming in BMECs monolayer can be evaluated by trans-endothelial electrical resistance (TEER) measurement and the trace of hydrophilic marker molecules that transport through the paracellular route. The sufficiently high TEER values and low permeability of the marker molecules are the indicators for *in vitro* BBB models to be considered adequate for drug transport studies (Malina et al., 2009; Wilhelm et al., 2011). The TEER values in a range of 150-200  $\Omega$ .cm<sup>2</sup> have been considered sufficient for the *in vitro* BBB models to proceed with the drug delivery studies (Deli et al., 2005; Tóth et al., 2011).

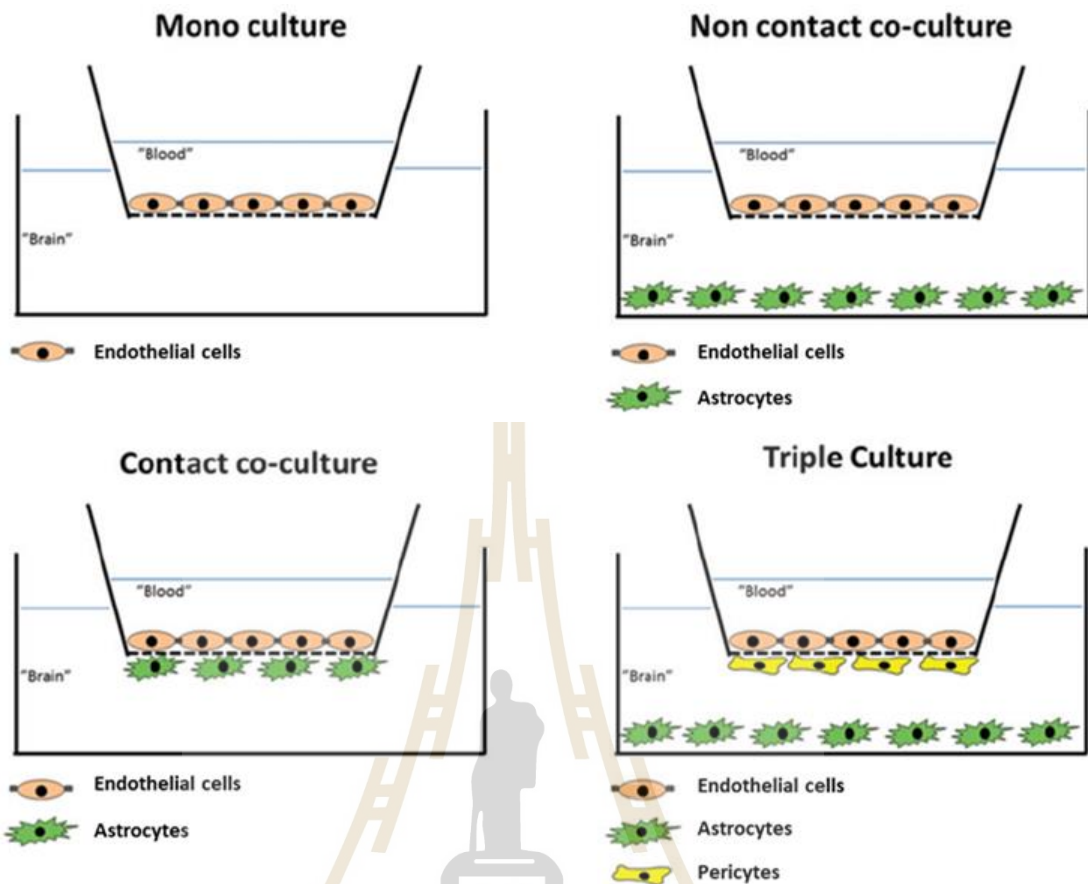
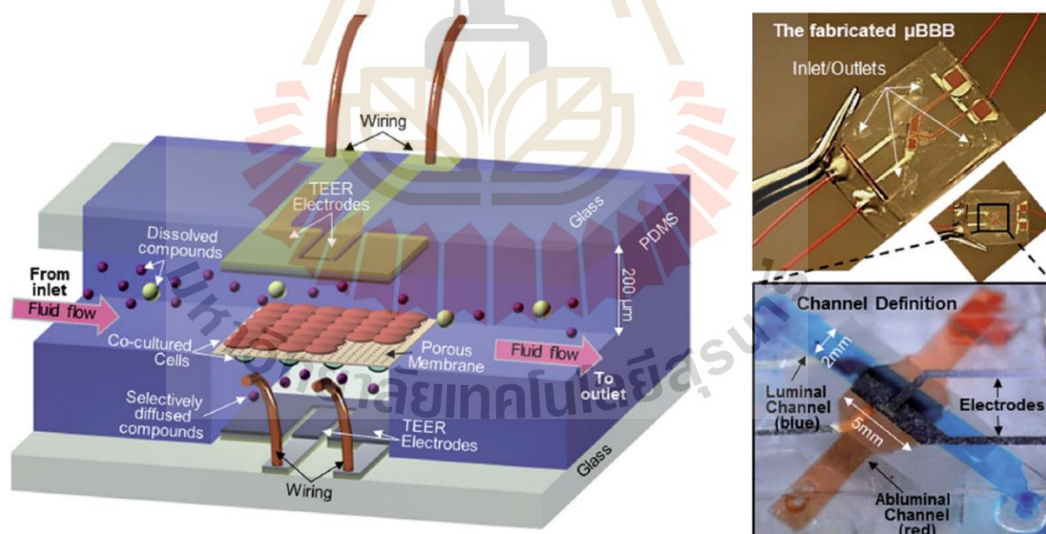


Figure 2.3 Schematic representation of monoculture and co-culture *in vitro* BBB models (Helms et al., 2016).

#### 2.2.2.2 Microfluidic *In vitro* BBB models (BBB-on-a-chip)

The microfluidic *in vitro* BBB models or BBB-on-a-chip have been developed to provide the dynamic system of BBB that imitate shear stress, which is the force generated by blood flow, resulting in closely resembling the realistic *in vivo* situation of the BBB (Chin and Goh, 2018). As shown in figure 2.4, the microfluidic BBB model consists of two perpendicular crossing channels, which are luminal (blue) and abluminal (red). The size of these channels was 200  $\mu\text{m}$  tall, 2 mm wide in the luminal channel, and 5 mm wide in the abluminal channel. A polycarbonate porous membrane separates the two channels of the model and also enables the co-culture of brain endothelial cells and astrocytes, which are seeded on the luminal and abluminal surfaces, respectively. The wiring of multiple built-in Ag/AgCl electrodes connects the

microfluidic BBB model to the Volt-Ohm meter to facilitate the measurement of TEER. The pumps and a gas tubing systems allow  $O_2$  and  $CO_2$  exchange and generate shear stress by allowing the dynamic flow of media through and around the channels of the model (Booth and Kim, 2012). The significant advantage of the microfluidic BBB model is that it provides the ability to monitor real-time BBB integrity, permeability, and cell imaging (Sivandzade and Cucullo, 2018). Moreover, co-culture with astrocytes of this model demonstrates high TEER values that can rise to  $\geq 250 \Omega \cdot \text{cm}^2$  (Booth and Kim, 2012). The different designs of BBB-on-a-chip are continuously developed to improve the modeling of BBB as close as the *in vivo* environment. Although the dynamic microfluidic models closely represent the physiological conditions of BBB, the elevation of complexity leads to a high cost, time-consuming, and requires technical expertise. These limitations made the microfluidic *in vitro* BBB models not suitable for high-throughput drug screening (Jackson et al., 2019).



**Figure 2.4** Schematic representation of microfluidic *in vitro* BBB model or BBB-on-a-chip (Booth and Kim, 2012).

### 2.3 Brain infectious diseases

Brain and spinal cord infections are serious, life-threatening diseases that continue to be concern globally. Brain infectious diseases can be characterized by infection areas of the brain such as meningitis (meninges), encephalitis (brain parenchyma), or brain abscess (brain parenchyma and extradural). The causative pathogens can be bacteria, viruses, parasites, or fungi that are able to cross the BBB and enter the CNS. The treatment of these diseases depends on rapid identification of the causative pathogens and selection of the right drugs with the effective concentration that can eliminate the pathogens within the CNS. However, there are difficulties to treat brain infections because of these three following obstacles: (1) limited access of antibiotics into the CNS due to the highly selective permeability of the BBB; (2) the antibiotics resistance development during treatments; and (3) the effect of immunomodulators (Ekizoğlu, 2017). Therefore, more studies are needed to find and develop effective treatments for brain infections.

Meningitis is one of the brain infections, which occurs when there is an inflammation of the membrane (meninges) surrounding the brain and spinal cord. The pathogens causing meningitis are bacteria (bacterial meningitis) and viruses (viral meningitis). In most cases, viral meningitis is considered to be the least deadly meningitis form compared to bacterial meningitis due to its mild symptoms and no significant long-term sequelae after recovery (Hoffman and Weber, 2009). For bacterial meningitis, it is a significant cause of infection-related deaths. Over 1.2 million cases of bacterial meningitis are estimated to occur worldwide each year (Borchorst and Moller, 2012). The incidence and mortality rates vary by age group, pathogen, region, country, immune status, and vaccination programs. The mortality rates can reach 70% if the patients have been left without treatment. Moreover, long-term sequelae such as neuron degeneration and permanent damage of the visual and hearing systems were found in 10-20% of the bacterial meningitis survivors (Edmond et al., 2010). The most common pathogens of bacterial meningitis are *Neisseria meningitidis*, *Listeria monocytogenes*, *Streptococcus pneumoniae*, and *Haemophilus influenzae* (Van de Beek et al., 2006). *H. influenzae* type b was once the leading cause of bacterial

meningitis in children. The development of the *H. influenzae* type b conjugate vaccine reduced the number of cases among children, whereas this type of bacterial meningitis still occurs in adults with immunocompromisation (Bisgard et al., 1998). *S. pneumoniae* is a common bacterial pathogen for meningitis in children and adults, especially the age under 5 years old and older than 60 years old. It was found to be the cause of death with 20-30% cases of hospital mortality (Weisfelt et al., 2006). *L. monocytogenes* is a common cause of bacterial meningitis in newborns, adults over 50 years old, immunodeficiency persons, and pregnant women. It can also cross the placenta barrier and lead to the fatal of the baby (Brouwer et al., 2006). Another pathogen that significantly causes bacterial meningitis worldwide with high morbidity and mortality is *N. meningitidis* (Rouphael and Stephens, 2012). The six of *N. meningitidis* serogroups, A, B, C, W135, X, and Y, were found to be responsible for meningococcal meningitis globally (Stephens, 2007). Infants, children, and adolescents are most vulnerable to being affected by this type of meningitis pathogen (MacNeil et al., 2018). Other bacteria that occasionally cause bacterial meningitis could be *Escherichia coli*, *Streptococcus agalactiae* (Group B streptococcus; GSB), *Pseudomonas aeruginosa*, *Klebsiella pneumoniae*, or methicillin-resistant *Staphylococcus aureus* (MRSA) (Pintado et al., 2011; Ekizoğlu, 2017). As shown in figure 2.5, the pathogenesis of bacterial meningitis begins with the colonization of the pathogens within the host nasopharynx. Then, the bacterial pathogens invade the mucosal barrier produced by epithelial cells and cross the vascular endothelium to enter the bloodstream. The bacteria replicate themselves within the blood to a high level, resulting in bacteremia. The expression of the thick capsule is one of the necessary mechanisms for the bacterial pathogens to defend the host's immune system and survive within the blood. Bacteria can penetrate the BBB through transcellular migration, paracellular migration, or invasion into white blood cells during transmigration ("Trojan-horse" mechanism), depending on the type of pathogens (Kim, 2008) (Figure 2.6). The penetration of bacterial pathogen across the BBB results in the elevation of the inflammatory mediators, including cytokines, chemokines, matrix metalloproteinases (MMPs), and reactive oxygen species (ROS) within the cerebrospinal fluid (CSF). This circumstance induces inflammation, BBB disruption, and recruitment of blood-borne neutrophils into the CNS (pleocytosis),

which leads to meningitis progression (Agyeman et al., 2017). However, the less common routes for bacteria to enter the CNS, such as the spreading from sinusitis and mastoiditis area, skull fracture, or ventricular shunts, can also cause meningitis (Kim, 2003).

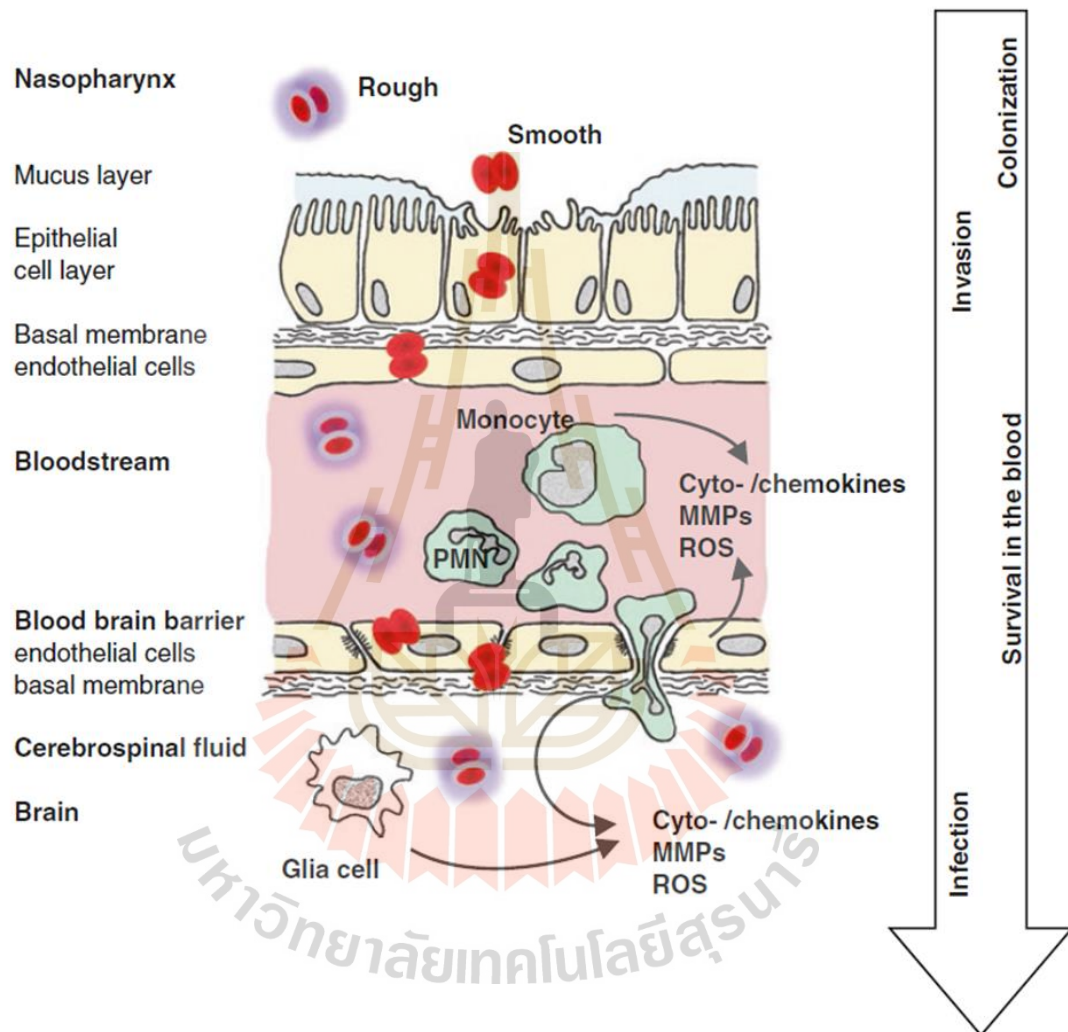
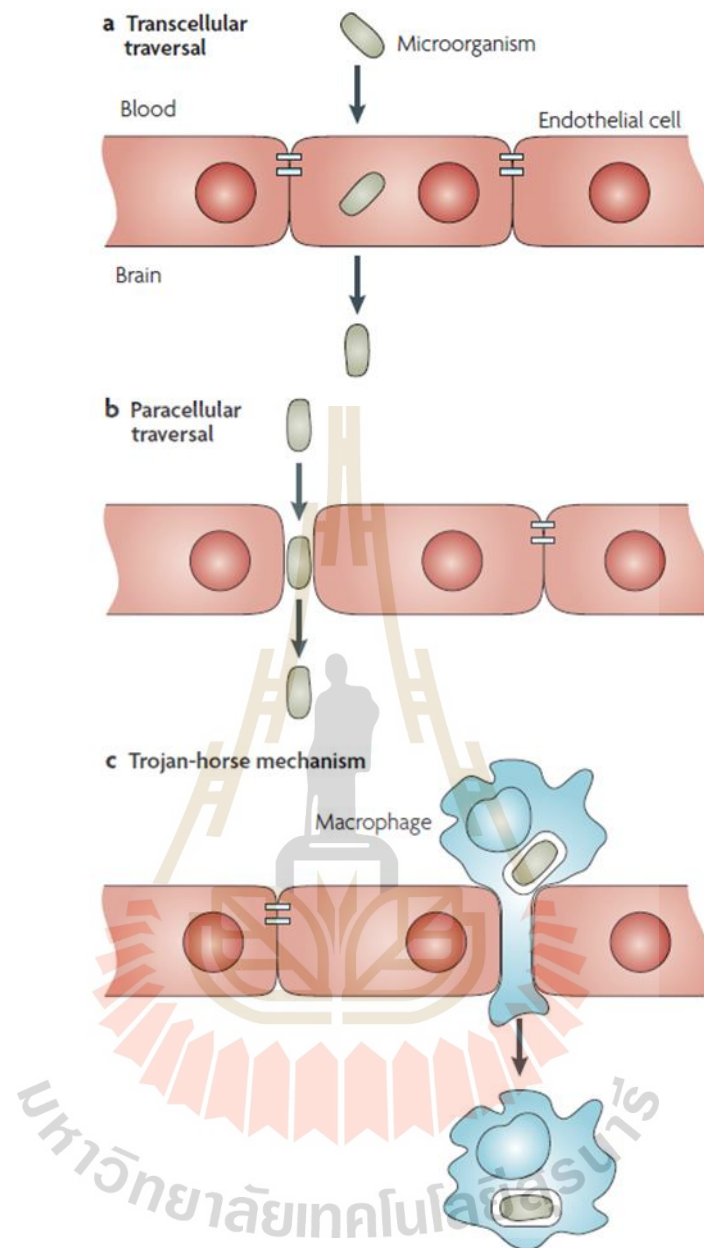


Figure 2.5 Pathogenesis of bacterial meningitis development (Agyeman et al., 2017).



**Figure 2.6** Mechanisms involved in the pathogen penetrate across the blood-brain barrier (Kim, 2008).

## 2.4 Allicin

Allicin (diallyl thiosulfinate) is a small lipophilic molecule that found to be the principal active compounds of freshly crushed garlic (Borlinghaus et al., 2014). “Allicin” was termed from the Latin name of the garlic plant, *Allium sativum*, and is also responsible for garlic’s characteristic pungent odor (Cavallito and Bailey, 1944). The precursor of allicin biosynthesis is the non-protein amino acid alliin (S-allyl-L-cysteine sulfoxide). The conversion of alliin to allicin occurs by the action of alliinase (E.C.4.4.1.4) enzyme. This reaction gives two products which are dehydroalanine and allyl sulfenic acid. Then, the two molecules of allyl sulfenic acid condense spontaneously to yield one molecule of allicin (Ilic et al., 2011) as showed in figure 2.7.

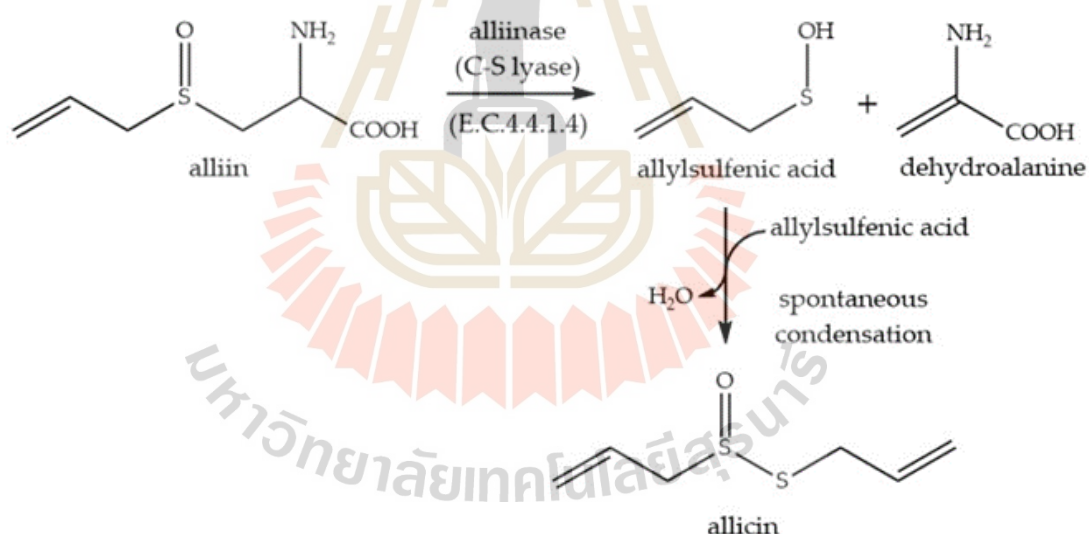


**Figure 2.7** Enzyme-catalyzed biosynthesis of allicin (Reiter et al., 2017).

In nature, allicin production is a potential defense mechanism against microbial pathogens of the soil. The garlic cloves are odor-free because of the different location of substrate alliin and the enzyme alliinase. The membrane which encloses the compartments that contain the substrate and enzyme would be destroyed upon the damage of garlic tissue by crushing or invading fungi or other soil pathogens. Therefore,

allicin would be rapidly produced and inactivate the invader. However, the massive production of allicin could be toxic for the plant tissues themselves. Thus, allicin possesses a short half-life and produces a limited amount to ensure that the clove defense mechanism remains in a very small location and a short period of time (Ellmore and Feldberg, 1994; Ankri and Mirelman, 1999). In the aqueous extract, allicin was most stable at pH 5-6 at room temperature (25°C) but rapidly degraded when the pH was above 11 or below 1.5, where allicin was completely degrading within 2 hours. The storage temperature also affects the stability of allicin. It rapidly degraded when the temperature was higher than 40°C. The half-life of allicin depends on its concentration, higher concentrations are more stable than lower concentrations. At room temperature, the half-life of allicin was approximately 15 days (Wang et al., 2014).

Allicin is a natural compound that possesses many different biological properties. Since ancient times, garlic has been used for medical therapeutic purposes. It has been reported to reduce blood lipid (Abramovitz et al., 1999) and lower blood pressure (Ried et al., 2008). Moreover, it has been demonstrated the anti-tumor activities which would be useful for cancer therapy and prevention (Hirsch, 2000). Several studies have been reported that allicin suppressed the proliferation of various types of cancer cells. The cytotoxic potential of allicin showed that allicin scored  $IC_{50}$  of 19.26  $\mu$ M, 28.51  $\mu$ M, 36  $\mu$ M, 77.92  $\mu$ M, 41.97  $\mu$ g/ml, and 6.23  $\mu$ g/ml on human hepatocellular cancer cell line HepG-2, human breast cancer cell line MCF-7, human lung cancer cell line A-549, human prostatic cancer cell line PC-3 (Ossama et al., 2019), human glioma cell line U251 (Li et al., 2018) and human glioblastoma cell line DBTRG-05MG (Weeranantanapan et al., 2020), respectively. Another significant property of allicin is antimicrobial activity. The effects of allicin have been investigated against a wide range of microorganisms including bacteria, fungi, protozoa, and viruses (Weber, 1992; Curtis et al., 2004). The antifungal activity of allicin was found to be useful for agricultural applications according to it inhibits the spore germination and hyphal growth of fungi (Curtis et al., 2004). Allicin can also be applied to medical therapy for the treatment of *Candida*-infections on the skin and aspergillosis in the lung (Shadkchan et al., 2004; Khodavandi et al., 2011). Moreover, allicin exhibited the antiparasitic effects on the protozoan parasite in the human intestinal tract, *Entamoeba histolytica* (Mirelman et

al., 1987). A recent proteome study demonstrated that allicin showed the antiviral and immunomodulatory activity in the human lung cell line Calu-3 infected with the Severe Acute Respiratory Syndrome Coronavirus 2 (SARS-CoV-2) (Mösbauer et al., 2021).

#### 2.4.1 Antibacterial properties of allicin

In 1944, Cavallito and Bailey were the first group who revealed that the antibacterial action of garlic is mainly due to allicin. Allicin exhibits a broad spectrum of antibacterial activity against Gram-negative and Gram-positive bacteria including species of *Escherichia*, *Salmonella*, *Klebsiella*, *Proteus*, *Bacillus*, *Streptococcus*, and *Staphylococcus* (Ankri and Mirelman, 1999). Allicin also has been reported the antibacterial effects on some of the most common meningitis pathogens. The minimum inhibitory concentration (MIC) and minimum bactericidal concentration (MBC) values for *L. monocytogenes* were 64 and 1,024 µg/ml allicin, respectively (Imani Rad et al., 2017). The MDR (multi-drug resistant) and non-MDR *S. pneumoniae* strains showed MICs ranging from 32 to 64 µg/ml allicin and MBCs from 64 to 128 µg/ml allicin (Reiter et al., 2017). The antibacterial effects of allicin against *N. meningitidis* were reported as percent of inhibitions, which were  $32 \pm 2.4\%$ ,  $76 \pm 4.8\%$ , and  $87 \pm 3.5\%$  at allicin concentrations of 100, 200, and 300 µg/ml, respectively (Shrivastava and Garg, 2015). Some antibiotic-resistant human pathogens were also shown to be susceptible to allicin such as Methicillin-resistant *Staphylococcus aureus* (MRSA). Interestingly, allicin was found to have a synergistic effect with certain antibiotics. For instance, streptomycin and chloramphenicol were discovered to have a synergistic effect with allicin against *Mycobacterium tuberculosis* (Gupta and Viswanathan, 1955). Moreover, most bacteria are unable to develop resistance to it due to the completely different mode of action from other antibiotics (Ankri and Mirelman, 1999).

#### 2.4.2 Mechanism of action of allicin on bacteria

The major mechanism involved in the antimicrobial effect of allicin is its interaction with essential thiol-containing enzymes in the microorganism. Allicin inactivates certain thiol-containing enzymes by the rapid reaction of thiosulfinates with thiol groups (Ankri and Mirelman, 1999). It specifically inhibits the bacterial enzyme such as acetate kinase and phosphotransacetyl-CoA synthetase in the acetyl-CoA-

forming system (Focke et al., 1990). Moreover, allicin was found to affect DNA, protein, and RNA synthesis in *Salmonella typhimurium* (Feldberg et al., 1988). The study in *E. coli* also suggested that RNA polymerase could be a target for allicin (Ozolin et al., 1990). Therefore, the multiple inhibitory effects of allicin on the various thiol-dependent enzymatic system are the reason for its broad-spectrum antimicrobial activities.

## 2.5 The possibility of allicin to cross the BBB

Kong et al. (2017) have investigated the neuroprotective effects of allicin on ischemia-reperfusion brain injury (IRBI) *in vivo*. The mice with allicin administration showed significantly reduced stroke size following IRBI compared to untreated mice. This study suggested that allicin may have the ability to pass BBB to attenuate the IRBI. A recent study on allicin's BBB penetrate ability was also reported by Itepu et al. (2019). They have constructed the 2D structure of allicin and its modified molecule to investigate their BBB penetration properties using the SwissADME server. The polar surface area (PSA), which is often used in medicinal chemistry to optimize the cell permeation ability of drugs, has been calculated. The study revealed that the PSA of allicin is 61.58 angstroms. The molecules that can penetrate the BBB should have PSA less than 90 angstroms (Hitchcock and Pennington, 2006). Thus, allicin is predicted to be able to pass BBB. Taken together, the results from these studies showed the possibility of allicin to cross the BBB. However, there is no direct evidence to clearly prove that allicin can pass through BBB.

## CHAPTER III

### MATERIALS AND METHODS

#### 3.1 Materials

##### 3.1.1 Bacterial strains and cell lines

The methicillin-resistant *Staphylococcus aureus* (MRSA) DMST20654, *Escherichia coli* TISTR780, *Escherichia coli* O157:H7 DMST12743, and the most common meningitis pathogens, including *Listeria monocytogenes* DMST20093 and *Neisseria meningitidis* ATCC13090 DMST7950 were purchased from the culture collection of the Department of Medical Sciences Thailand (DMST) and Thailand Institute of Scientific and Technological Research (TISTR). Meningitis pathogens were cultured in Tryptic soy broth (TSB), and other strains were cultured in Mueller Hinton broth (MHB) at 37°C for 24 h.

The hCMEC/D3, which is the brain microvascular endothelial cell line, was purchased from the American Type Culture Collection (Merck Millipore, MO, USA). This cell line was used to construct the BBB model *in vitro*. The cells were grown in EMB-2 medium containing growth factors and antibiotics (gentamicin sulfate and amphotericin-B) on a collagen-coated flask. The cultured cells were incubated at 37°C in a humidified incubator with 5% CO<sub>2</sub>.

##### 3.1.2 Media and reagents

###### 3.1.2.1 Bacterial culture media

Mueller Hinton (MH) medium (Himedia, India) contained beef extract 2 g/l, casein hydrolysate 17.5 g/l, and starch 1.5 g/l (pH 7.4 ± 0.2).

Tryptic soy (TS) medium (Himedia, India) contained tryptone (pancreatic digest of casein) 17 g/l, soya peptone 3 g/l, sodium chloride 5 g/l, dipotassium hydrogen phosphate 2.5 g/l, and dextrose 2.5 g/l (pH 7.3 ± 0.2).

The solid medium was prepared by adding 15 g into the medium 1 liter. All the media were sterilized by autoclaving at 121°C for 20 min.

### 3.1.2.2 Cell culture media

Endothelial cell growth basal medium-2 (EBM-2), supplements, and growth factors were purchased from Lonza (Walkersville, MD, USA). The 1X EBM-2 medium was prepared by adding the growth factors and supplements (25 ml FBS; Fetal bovine serum, 0.2 ml hydrocortisone, 2 ml hFGF-B; Human fibroblastic growth factor-basic, 0.5 ml VEGF; Vascular endothelial growth factor, 0.5 ml R<sup>3</sup>IGF-1; Recombinant long R insulin-like growth factor-1, 0.5 ml ascorbic acid, 0.5 ml hEGF; Human epidermal growth factor, and 0.5 ml GA-1,000; Gentamicin sulfate-Amphotericin-B) into 500 ml basal medium. Then, the culture medium was stored at 4°C until used.

### 3.1.2.3 Allicin

Allicin (purity >98%) was purchased from Abcam (USA). The stock solution of allicin (1 mg/ml) was prepared by dissolving in absolute ethanol (RCI Labscan, Thailand). Then, the stock allicin was aliquot and stored at -20°C until used. The new aliquot of stock allicin was used in the individual experiment.

### 3.1.2.4 Collagen Type I, Rat tail

Collagen Type I, Rat tail (extracted from rat tail tendons) was purchased from EMD Millipore (Billerica, MA, USA) and stored at 2-8°C until used.

### 3.1.2.5 MTT

MTT (3-(4,5-dimethylthiazol-2-yl)-2,5-diphenyltetrazolium bromide) powder was purchased from Invitrogen (Eugene, OR, USA) and stored at -25-30°C until used.

### 3.1.2.6 Hanks' Balanced Salt Solution (HBSS)

The sterile HBSS (1X) was purchased from Gibco (NY, USA) and stored at 15-30°C until used.

### 3.1.2.7 Dulbecco's phosphate buffered saline (DPBS)

The sterile DPBS was purchased from Millipore (USA) and stored at 25°C until used.

### 3.1.2.6 Lucifer yellow (LY)

Lucifer yellow CH dipotassium salt powder was purchased from Sigma (St. Louis, MO, USA) and stored at 25°C until used.

## 3.2 Methods

### 3.2.1 Minimum inhibitory concentration (MIC) assay

In order to determine the minimum inhibitory concentration (MIC) of allicin for each bacterial pathogen, the broth microdilution assay was performed. Each strain was streaked onto MHA plates (or TSA; Tryptic soy agar for meningitis pathogens) and incubated for 24 h at 37°C. The colonies were selected using a sterile cotton swab and transferred into a sterilized tube containing sterile MHB (or TSB; Tryptic soy broth for meningitis pathogens). The turbidity was verified by measuring the absorbance of the inoculum spectrophotometrically. The absorbance was in the same range as 0.5 McFarland standard ( $OD_{625\text{ nm}}$  approximately at 0.08–0.13). Then, diluted the inoculum 1:100 in broth and transferred 50  $\mu\text{l}$  of the bacterial suspension into a 96-well microplate containing 50  $\mu\text{l}$  of various concentrations of allicin in a range of 0.5 to 50  $\mu\text{g/ml}$ . The final inoculum density would be approximately  $5 \times 10^5$  CFU/ml. The growth control well was filled with 50  $\mu\text{l}$  of broth and 50  $\mu\text{l}$  of the bacterial suspension. The sterility control well was filled with 100  $\mu\text{l}$  of broth. The experiments were repeated in triplicate. Afterward, the plates were incubated for 20-24 h at 37°C. After incubation, the lowest concentration of allicin that inhibits the visible growth of the bacterial pathogens was determined as MIC value.

### 3.2.2 Cell viability assay

Cell viability of hCMEC/D3 cells was examined using an MTT assay. The yellow MTT (3-(4,5-dimethylthiazol-2-yl)-2,5-diphenyltetrazolium bromide) is reduced

to purple formazan form by the action of mitochondria succinate dehydrogenase enzymes in living cells. The quantity of formazan is proportional to the number of viable cells. The hCMEC/D3 cells were seeded in 96-well plates at a density of  $1 \times 10^4$  cells/well for 24 h. Then, the cells were treated with 100  $\mu$ l of allicin at concentrations of 0.5, 1, 2, 5, and 10  $\mu$ g/ml for 3 h. After allicin removal, 10  $\mu$ l of MTT reagent (5 mg/ml) and 100  $\mu$ l of PBS were added to each well and incubated for 4 h. After MTT removal, 50  $\mu$ l of DMSO was added to solubilize the formazan crystals. The optical density (OD) was measured at a wavelength of 540 nm using the microplate reader. The experiments were repeated in triplicate.

### 3.2.3 The construction of the *in vitro* BBB model

The *in vitro* model of BBB was generated using a transwell system that consists of the upper (apical or AP) and lower (basolateral or BL) chambers which imitate the blood and brain side of the BBB, respectively (Fig 3.1). The two chambers of the insert are separated by a porous membrane (0.4  $\mu$ m). Firstly, the 24-well inserts (Millicell, Germany) were coated with collagen 1:20 in Dulbecco's phosphate-buffered saline (DPBS) at 200  $\mu$ l/well and incubated at 37°C and 5% CO<sub>2</sub> for 40-60 min. After collagen removal, the hCMEC/D3 cells were seeded on the collagen-coated membrane of the insert at a density of  $1 \times 10^4$  cells/well. The cell-free inserts, which are collagen-coated and non-collagen-coated, were also used as control inserts. Then, the apical and basolateral chambers of the BBB model were filled with the Endothelial cell growth basal medium-2 (EMB-2) medium at 200  $\mu$ l and 1,000  $\mu$ l, respectively. The cells were cultured for approximately 21 days at 37°C and 5% CO<sub>2</sub>. The culture medium in both AP and BL chambers was carefully changed every 3 days from 1X to 0.5X and 0.25X during the culture period. The number of X refers to the concentration of the growth factors and supplements that were added into the culture medium. On day 21, TEER (Trans-endothelial electrical resistance) measurement and lucifer yellow assay were performed to verify the integrity of the BBB model *in vitro*.

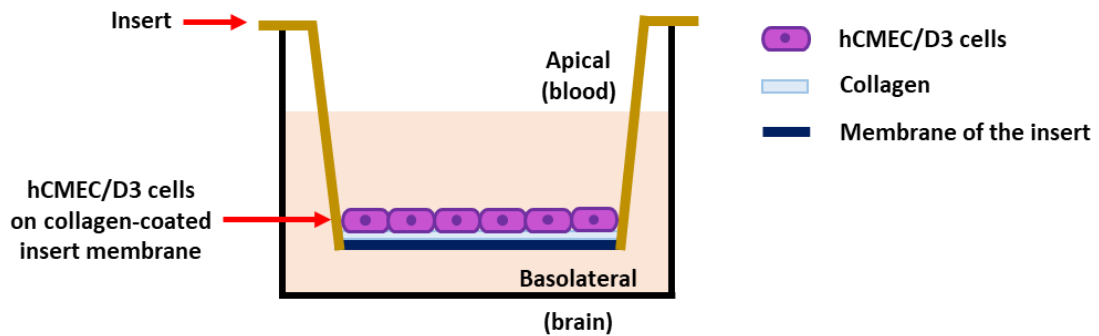


Figure 3.1 The *in vitro* BBB model (modified from Wolff et al., 2015)

### 3.2.3.1 Trans-endothelial electrical resistance measurement (TEERs)

To confirm the integrity and permeability of the endothelial monolayer of the *in vitro* BBB model using a TEER measurement system known as an Epithelial Voltohmmeter (EVOM2) with chopstick electrode STX2, each stick of the electrode pair was placed in the AP and BL chambers to measure the electrical resistance across an endothelial monolayer. The measurement process includes measuring the blank resistance ( $R_{\text{Blank}}$ ) of the membrane without cells and measuring the resistance across the cell layer on the membrane ( $R_{\text{Total}}$ ). The cell-specific resistance ( $R_{\text{Tissue}}$ ) in units of  $\Omega$ , was obtained as:

$$R_{\text{Tissue}} (\Omega) = R_{\text{Total}} - R_{\text{Blank}}$$

The TEER values are typically reported ( $\text{TEER}_{\text{Reported}}$ ) in units of  $\Omega \cdot \text{cm}^2$  and calculated as:

$$\text{TEER}_{\text{Reported}} = R_{\text{Tissue}} (\Omega) \times \text{Area of the membrane (cm}^2\text{)}$$

### 3.2.3.2 Lucifer yellow permeability assay

Lucifer yellow (LY) assay allows measuring the endothelial layer permeability by monitoring the passage of LY across the *in vitro* BBB model. Firstly, all media was removed from the apical and basolateral chambers of the inserts. Then, 200  $\mu\text{l}$  of LY (20  $\mu\text{M}$ ) and 1,000  $\mu\text{l}$  of HBSS were added into AP and BL chambers, respectively. After incubation for 1 h at 37°C and 5%  $\text{CO}_2$ , the samples were collected.

The concentration of LY from the BL chamber of the inserts was measured using a fluorescence microplate reader with excitation at 485 nm and emission at 530 nm. The %LY rejection of the *in vitro* BBB model was calculated using the equation (Nkabinde et al., 2012) below:

$$\%LY \text{ rejection} = \left(1 - \frac{\text{LY concentration in BL chamber}}{\text{Initial concentration of LY}}\right) \times 100$$

### 3.2.4 Determination of allicin in the *in vitro* BBB model by HPLC analysis

According to the cell viability assay results, the non-toxicity concentrations of allicin (0.5, 1, 2, and 5 µg/ml) were selected. After verifying the *in vitro* BBB model by TEER measurement and LY assay, the allicin test was carried out by adding 200 µl of the selected concentrations of allicin and 1,000 µl of HBSS into the apical and basolateral chambers of the inserts, respectively. Simultaneously, the cell-free control inserts, which are collagen-coated and non-collagen-coated, were also treated with 200 µl of allicin 5 µg/ml. After incubation for 3 h at 37°C and 5% CO<sub>2</sub>, the samples were collected. The LY assay and TEER measurement were performed again, respectively to confirm that the integrity of the *in vitro* BBB model before and after the allicin test is still intact. The concentrations of allicin that can cross the endothelial layer from AP to BL chamber were analyzed by high-performance liquid chromatography (HPLC) analysis. The HPLC system consisted of the following components: A pump, an injector, a hypersil ODS column (250 x 4.0 mm, 5 µm particle size), and a UV detector (254 nm). The column operated in isocratic mode (50:50 MeOH: H<sub>2</sub>O) at a 0.5 ml/min flow rate. The standard concentrations of allicin and HBSS, which is the solvent of allicin, were also analyzed by HPLC analysis. Allicin concentrations of 0.5, 1, 1.5, 2, 3, 4, and 5 µg/ml were used to generate a standard curve for determining the concentration of samples from the *in vitro* BBB model. The chromatogram from HPLC analysis showed the different peaks or patterns of the components in the sample. The peak of allicin was detected by comparing the chromatogram of the samples to the chromatogram of HBSS (baseline). The peak area

of allicin refers to the concentration of allicin in the samples according to the standard curve.

### 3.2.5 Cellular uptake experiments

In order to investigate the ability of the hCMEC/D3 cells in allicin uptake, cellular uptake experiments were performed. The experiments consisted of two conditions: (1) with cells and (2) without cells. In the first condition (with cells), the hCMEC/D3 cells were seeded in the collagen-coated wells of the 24-well plate at a density of  $1 \times 10^4$  cells/well. Simultaneously, one well was also seeded with hCMEC/D3 cells at a density of  $5 \times 10^4$  cells/well to investigate whether the increases in the cells number would increase the allicin uptake. The second condition (without cells) was filled with a cell-free medium. All wells were filled with 500  $\mu$ l of culture medium and incubated for 24 h at 37°C and 5% CO<sub>2</sub>. Afterward, the culture medium was removed from the plate. Then, 250  $\mu$ l of the non-toxicity concentrations of allicin, which are 0.5, 1, 2, and 5  $\mu$ g/ml, were added into the wells with cells ( $1 \times 10^4$  cells/well) and without cells. However, the well with a cell density of  $5 \times 10^4$  cells/well was treated with only 250  $\mu$ l of 5  $\mu$ g/ml allicin. After incubation for 3 h at 37°C and 5% CO<sub>2</sub>, the supernatants were collected and analyzed to determine the allicin concentration by HPLC analysis.

### 3.2.6 Statistical analysis

The experiments were performed in triplicates. Data were expressed as the mean  $\pm$  standard error of the mean (SEM). The statistical difference in the cell viability of hCMEC/D3 cells after allicin treatment relative to control was carried out by using a one-way analysis of variance (one-way ANOVA) followed by Bonferroni's post hoc test. The significant difference between the allicin concentration in the presence and absence of hCMEC/D3 cells was compared by using an independent *t*-test. The *p*-value of <0.05 was used to indicate a statistical significance.

## CHAPTER IV

### RESULTS AND DISCUSSION

#### 4.1 Minimum inhibitory concentration (MIC) values of allicin against bacterial pathogens

Antibacterial activity of allicin was examined by using the broth microdilution method to determine the minimum inhibitory concentration (MIC) of allicin for individual bacterial pathogens. The results showed that MIC values of allicin ranged from 3 to 30 µg/ml. Allicin exhibited the strongest antibacterial activity against *N. meningitidis* ATCC13090 DMST7950 with the MIC value of 3 µg/ml. The weakest antibacterial activity of allicin was observed against *L. monocytogenes* DMST20093 with the MIC value of 30 µg/ml (Table 4.1). These results revealed that *N. meningitidis* was the most sensitive to allicin.

**Table 4.1** The MIC values of allicin against bacterial pathogens.

Bacterial pathogens	MICs (µg/ml)
<i>N. meningitidis</i> ATCC13090 DMST7950	3
<i>L. monocytogenes</i> DMST20093	30
<i>E. coli</i> TISTR780	25
<i>E. coli</i> O157:H7 DMST12743	25
MRSA DMST20654	15

According to the evidence that allicin exhibited a broad spectrum of antibacterial activity against Gram-positive and Gram-negative bacteria (Ankri and Mirelman, 1999) including some of the meningitis pathogens. In this study, the antibacterial activity of allicin was investigated against two of the most common meningitis bacteria, which are *N. meningitidis* and *L. monocytogenes*, including other bacteria, which occasionally be the causative pathogens of bacterial meningitis. *E. coli*, a Gram-negative bacterium, is

regularly found as a cause of meningitis among neonates, infants, the elderly, and immunocompromised people (Ekizoğlu, 2017). Methicillin-resistant *Staphylococcus aureus* (MRSA) is a Gram-positive bacterium that rarely causes bacterial meningitis, but the symptoms could be severe and lead to death. MRSA meningitis occurred in patients who received recent neurosurgery or acquired cerebrospinal fluid (CSF) devices (Pintado et al., 2011). The previous study has been reported that MIC values of allicin against *E. coli* and *L. monocytogenes* were 32 and 64 µg/ml, respectively (Imani Rad et al., 2017), whereas the obtained results showed the lower MICs in *E. coli* (25 µg/ml), the pathogenic form *E. coli* O157:H7 (25 µg/ml) and *L. monocytogenes* (30 µg/ml). According to this finding, this study could define the MIC value more precisely due to the tested concentration of allicin was in a range of 0.5 – 50 µg/ml, while their study used 2-fold serial dilutions of allicin in a range of 2 – 1,024 µg/ml. Cutler and Wilson (2004) have investigated the effect of allicin against 30 clinical isolates of MRSA and revealed that 88% of strains had MICs at 16 µg/ml, and all strains were inhibited at 32 µg/ml. In comparison to the present study, the obtained result showed the correlated MICs of allicin against MRSA (15 µg/ml) with their majority tested strains. Moreover, this study provided the first evidence that the MIC value of allicin against *N. meningitidis* was 3 µg/ml. The Gram-negative *N. meningitidis* is a significant cause of bacterial meningitis globally. In spite of effective antibiotics (e.g., cephalosporin; cefotaxime or ceftriaxone, Penicillin G, ampicillin, chloramphenicol, fluoroquinolone, and aztreonam) and partially effective vaccines, the prevention of the infection with *N. meningitidis* is still challenging (Tzeng and Stephens, 2000; Tunkel et al., 2004). According to the results from this study, allicin inhibited the growth of *N. meningitidis* with a low MIC value compared to other tested pathogens. Therefore, in case allicin is proved to be able to cross the BBB, it will be beneficial for the treatment of meningitis caused by *N. meningitidis*.

## 4.2 The cytotoxicity of allicin on hCMEC/D3 cells

According to the MIC method, the doses of allicin that inhibited the growth of meningitis pathogens were revealed. To propose allicin as a therapeutic candidate for meningitis treatment, the cytotoxicity dose of allicin on the BBB cells used in this study, which is hCMEC/D3 cells, was also determined. In order to investigate the effect of allicin on the cell viability of hCMEC/D3 cells, the MTT assay was performed. The result showed that allicin at a concentration of 10  $\mu\text{g/ml}$  significantly reduced the cell viability compared to the untreated control group ( $p < 0.05$ ). The highest non-toxicity concentration of allicin on hCMEC/D3 cells was 5  $\mu\text{g/ml}$  (Figure 4.1). Therefore, the non-toxicity concentrations of allicin (0.5, 1, 2, and 5  $\mu\text{g/ml}$ ) were selected to further investigate the ability of allicin to cross the *in vitro* BBB model.

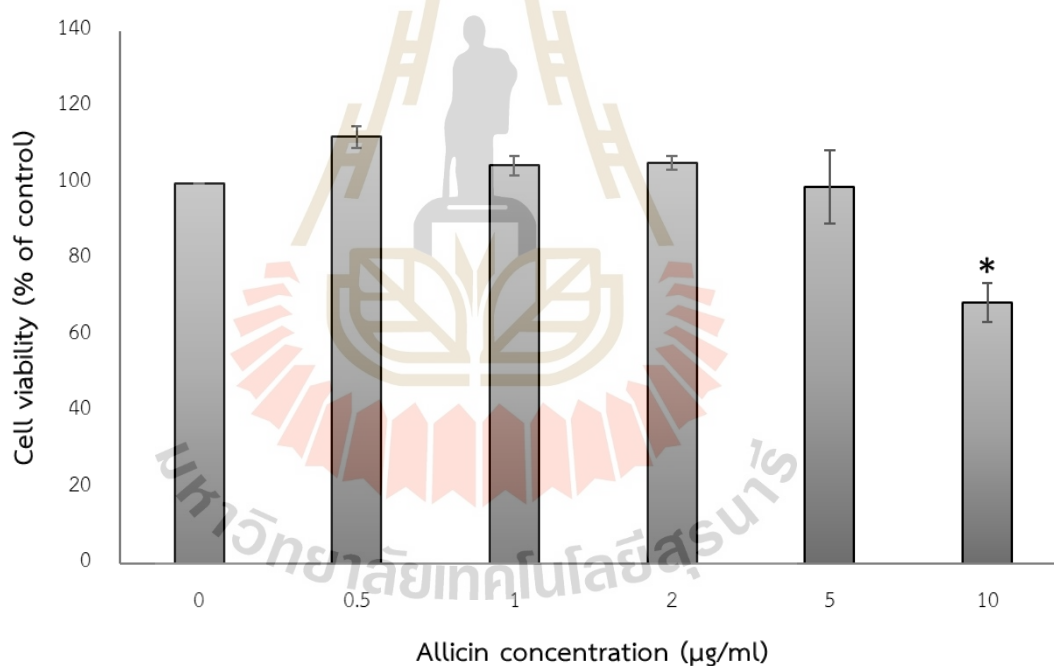


**Figure 4.1** The cytotoxicity of allicin on hCMEC/D3 cells. The cells were treated with various concentrations of allicin (0-10  $\mu\text{g/ml}$ ) for 3 h. Then, the cell viability was measured by MTT assay. The percentage of cell viability compared with the untreated control. The values were expressed as mean  $\pm$  SEM ( $n=3$ ). \*  $p < 0.05$  compared with the untreated control.

### 4.3 The ability of allicin to cross the *in vitro* BBB model

In order to investigate the ability of allicin to cross the *in vitro* BBB model, the construction of *in vitro* BBB model was the first process of experiments. The monoculture BBB model in which only hCMEC/D3 cells are grown on the collagen-coated membrane of the transwell insert was used in this study. The *in vitro* BBB model was divided into two compartments, which are the apical (AP) and basolateral (BL) chambers (Figure 3.1 in chapter III) that mimic the blood and brain side of the BBB, respectively. The cells were grown to form a confluent monolayer; then, TEER measurement and LY assay were performed before and after the allicin test to verify the integrity and permeability of the BBB model *in vitro*.

The results of the TEER measurement showed that the average TEER value of the *in vitro* BBB models before the allicin test was  $14.43 \pm 1.2 \Omega \cdot \text{cm}^2$  and slightly decreased to  $10.33 \pm 0.5 \Omega \cdot \text{cm}^2$  after the allicin test. The previous study has been reported that TEER values of hCMEC/D3 monolayer under static culture conditions were approximately 30 – 50  $\Omega \cdot \text{cm}^2$  (Weksler et al., 2013). In comparison to the obtained results, TEER values in the present study were lower than the desired value.

Because the obtained TEER values were lower than expected, the LY assay was performed to ensure the integrity of the *in vitro* BBB model. The results showed that the average %LY rejection of the *in vitro* BBB models before the allicin test was  $97.61 \pm 0.3\%$ . To our best knowledge, there was no available report of %LY rejection value which indicates the intactness of the hCMEC/D3 monolayer. Himanshu et al. (2013) have reported that the %LY rejection values >99% suggested that the integrity of the Caco-2 monolayer was intact. In comparison, the obtained %LY rejection value was lower than the criteria of Caco-2 cells, which are the epithelial cell line of colon carcinoma. The possible reason underlying this circumstance might be the original location of the cells. The hCMEC/D3 cells, derived from the brain, are more vulnerable than the cells in the intestine. However, the previous study also reported that the Caco-2 monolayer with an average TEER value of 250  $\Omega \cdot \text{cm}^2$  (intact monolayers) showed the %LY rejection value of  $96.88 \pm 0.2\%$  at day 21 (Nkabinde et al., 2012), which is consistent with the obtained results. Taken together, although TEER values of

the *in vitro* BBB models before the allicin test were lower than the desired value, the obtained %LY rejections in this study were considered intact. The principle of the LY assay was measuring the permeability by directly monitoring the passage of LY across the hCMEC/D3 monolayer. Hence, the %LY rejections were considered more reliable than TEER values. Therefore, the results of %LY rejection indicated that the *in vitro* BBB models were efficient to proceed with the allicin test. Moreover, the integrity of the *in vitro* BBB model after performing the allicin tests was also verified and showed that the %LY rejection was slightly decreased to  $95.04 \pm 1.3\%$ . Although the %LY rejection at the end of the allicin test was reduced, the present study showed that there was no leakage of allicin into the BL chamber of the *in vitro* BBB model (Figure 4.3), suggesting that the integrity of the hCMEC/D3 monolayer was acceptable.

After allicin testing via the *in vitro* BBB model, HPLC analysis was used to determine the concentration of allicin that crosses the hCMEC/D3 monolayer from AP to BL chamber of the *in vitro* BBB model. The standard allicin (0.5-5  $\mu\text{g/ml}$ ) and HBSS (blank) were the first to be analyzed. Then, the peak of allicin was detected by comparing the chromatogram of the standard allicin to the baseline chromatogram of HBSS. As shown in Figure 4.2B-H, the retention time of the allicin peak was approximately 8.7 min. Due to the peak area referring to the concentration of allicin in the sample, the size of the peak area was proportional to the concentration of the standard allicin (arrows). According to these results, the standard curve of allicin was established and the correlation coefficient was 0.999 (Appendix B).

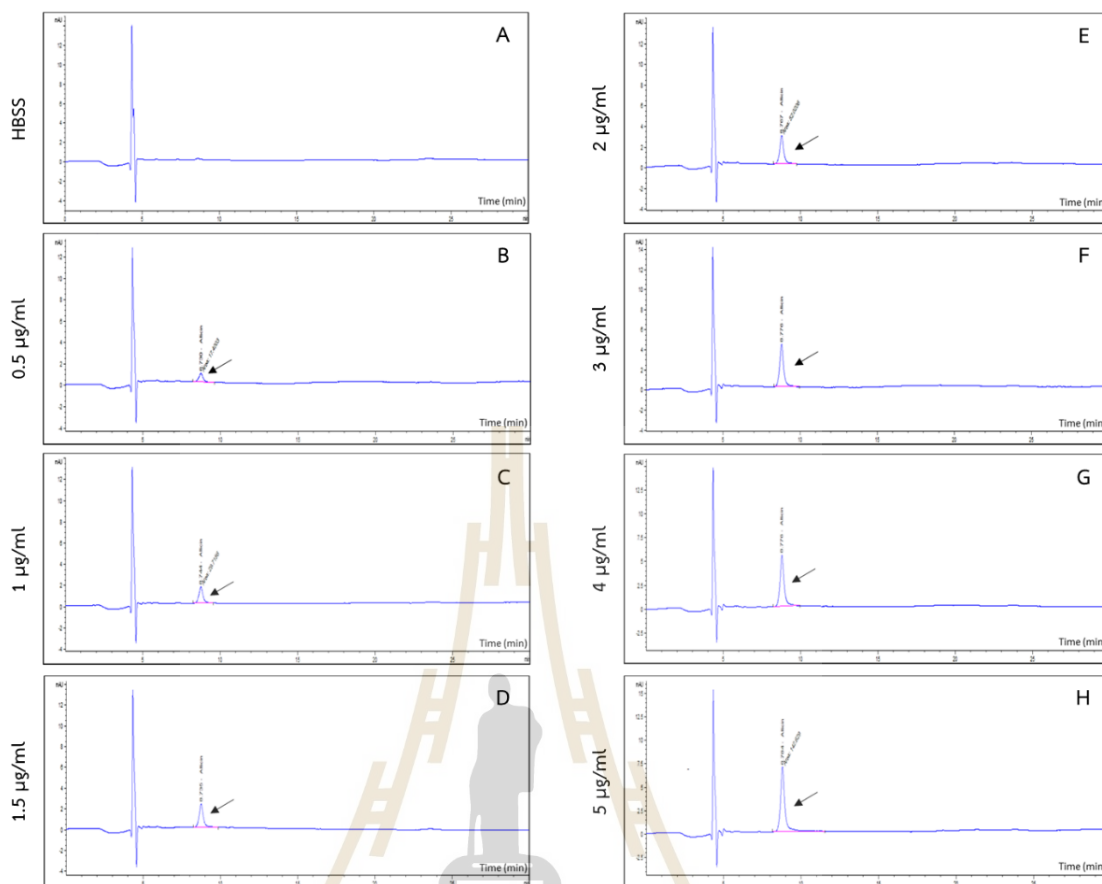


**Figure 4.2** HPLC analysis of HBSS (baseline) and standard alliin. (A) Chromatogram of HBSS. (B-H) Chromatogram of standard alliin 0.5, 1, 1.5, 2, 3, 4, and 5  $\mu\text{g/ml}$ , respectively.

Surprisingly, the HPLC analysis results of the samples from AP and BL chambers of the *in vitro* BBB model showed that alliin peak did not appear in either AP and BL samples tested with alliin 0.5, 1, 2, and 5  $\mu\text{g/ml}$  (Figure 4.3).

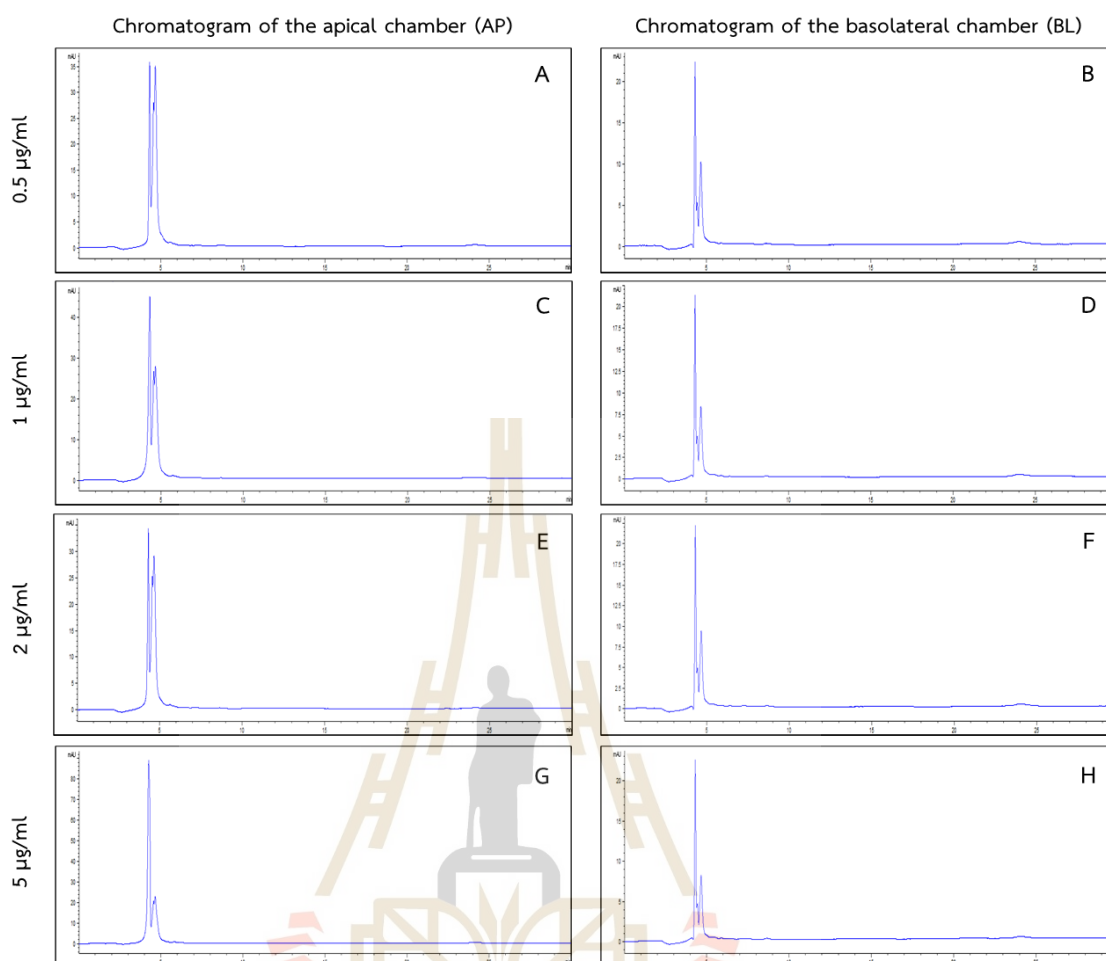


**Figure 4.3** HPLC analysis of allicin samples from the *in vitro* BBB model. (A-B) Chromatogram of AP and BL samples tested with allicin 0.5 µg/ml. (C-D) Chromatogram of AP and BL samples tested with allicin 1 µg/ml. (E-F) Chromatogram of AP and BL samples tested with allicin 2 µg/ml. (G-H) Chromatogram of AP and BL samples tested with allicin 5 µg/ml.

On the contrary, the allicin peak was detected in the AP and BL samples from the cell-free control inserts, which are collagen-coated and non-collagen-coated, tested with allicin 5 µg/ml (Figure 4.4 and 4.5). Moreover, the peak area of allicin from the collagen-coated and non-collagen-coated control inserts was similar in size on both AP and BL samples, resulting in similarly calculated allicin concentration. The allicin concentration of AP from the collagen-coated and non-collagen-coated control inserts

were 1.97 and 1.72  $\mu\text{g/ml}$ , respectively, while the allicin concentration of BL from the collagen-coated and non-collagen-coated control inserts were 1.09 and 1.11  $\mu\text{g/ml}$ , respectively (Table 4.2 and 4.3).

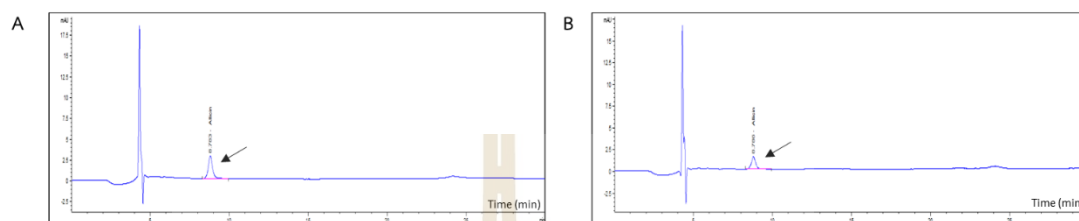


**Figure 4.4** HPLC analysis of allicin samples from the collagen-coated control insert (cell-free) tested with allicin 5  $\mu\text{g/ml}$ . (A) Chromatogram of AP samples (B) Chromatogram of BL samples.

**Table 4.2** Peak area and allicin concentration of AP and BL samples of the collagen-coated control insert.

Sample	Peak area of allicin (mAU*s)	Allicin concentration ( $\mu\text{g/ml}$ )
AP of the collagen-coated control insert	53.78	1.97
BL of the collagen-coated control insert	29.69	1.09

Abbreviation: mAU: milli-Absorbance Units, s: second.

Each value was obtained from n=1 experiment.

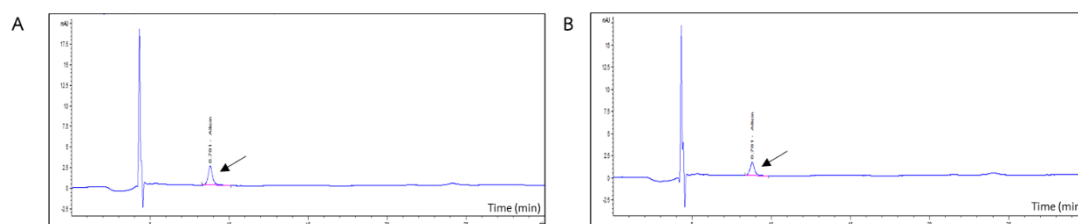


**Figure 4.5** HPLC analysis of alliin samples from the non-collagen-coated control insert (cell-free) tested with alliin 5  $\mu\text{g}/\text{ml}$ . (A) Chromatogram of AP samples (B) Chromatogram of BL samples.

**Table 4.3** Peak area and alliin concentration of AP and BL samples of the non-collagen-coated control insert.

Sample	Peak area of alliin (mAU*s)	Alliin concentration ( $\mu\text{g}/\text{ml}$ )
AP of the non-collagen-coated control insert	47.08	1.72
BL of the non-collagen-coated control insert	30.26	1.11

Abbreviation: mAU: milli-Absorbance Units, s: second.

Each value was obtained from n=1 experiment.

Interestingly, the triplicate results of HPLC analysis were consistent that alliin peak was not detected in the AP and BL samples of the *in vitro* BBB model. The temperature used in the alliin test (37°C) was suspected to be one of the factors responsible for alliin degradation at the end of the experiments. To prove this possibility, the temperature test was performed by incubating the opened cap eppendorf containing alliin at a concentration of 5  $\mu\text{g}/\text{ml}$  at 37°C for 3 h. The results from HPLC analysis showed that the alliin peak was detected, and the concentration of alliin in the sample was approximately  $4.91 \pm 0.7 \mu\text{g}/\text{ml}$  (Appendix C), which is similar to the initial

concentration of allicin (5 µg/ml) before temperature test. Moreover, the previous studies revealed that allicin rapidly degraded when the temperature was higher than 40°C (Wang et al., 2014). Tanongkankit et al. (2019) also reported that the half-life period of allicin at 40°C was 3 days, which the temperature and time were higher and longer than the allicin test condition (37°C and 3 h) in this present study. These findings suggested that allicin did not degrade during the allicin test. Thus, the disappearance of allicin might occur due to the structure of the *in vitro* BBB model. At least, the allicin peak was expected to be detected in AP samples due to a higher allicin concentration than BL samples, whereas the results were inconsistent with the prediction. Therefore, this finding led to the hypothesis that allicin, which is supposed to move across the hCMEC/D3 monolayer from AP to BL chamber, might be trapped in some part of the *in vitro* BBB model. Thus, the 3 possibilities of where allicin localized after testing via the *in vitro* BBB model was proposed: (1) Allicin was uptaken into hCMEC/D3 cells (2) Allicin was trapped in the collagen, and (3) Allicin was trapped in the membrane of the insert (Figure 4.6).

As previously mentioned, the obtained results revealed that the allicin peak was detected in both AP and BL samples from the collagen-coated and non-collagen-coated inserts (Figure 4.4 and 4.5, Table 4.2 and 4.3). This finding demonstrated that the absence of allicin in the *in vitro* BBB model was probably not due to allicin being trapped in the collagen or membrane of the insert. Consequently, the remaining hypothesis, which allicin was uptaken by hCMEC/D3 cells, would be further investigated using cellular uptake experiments.

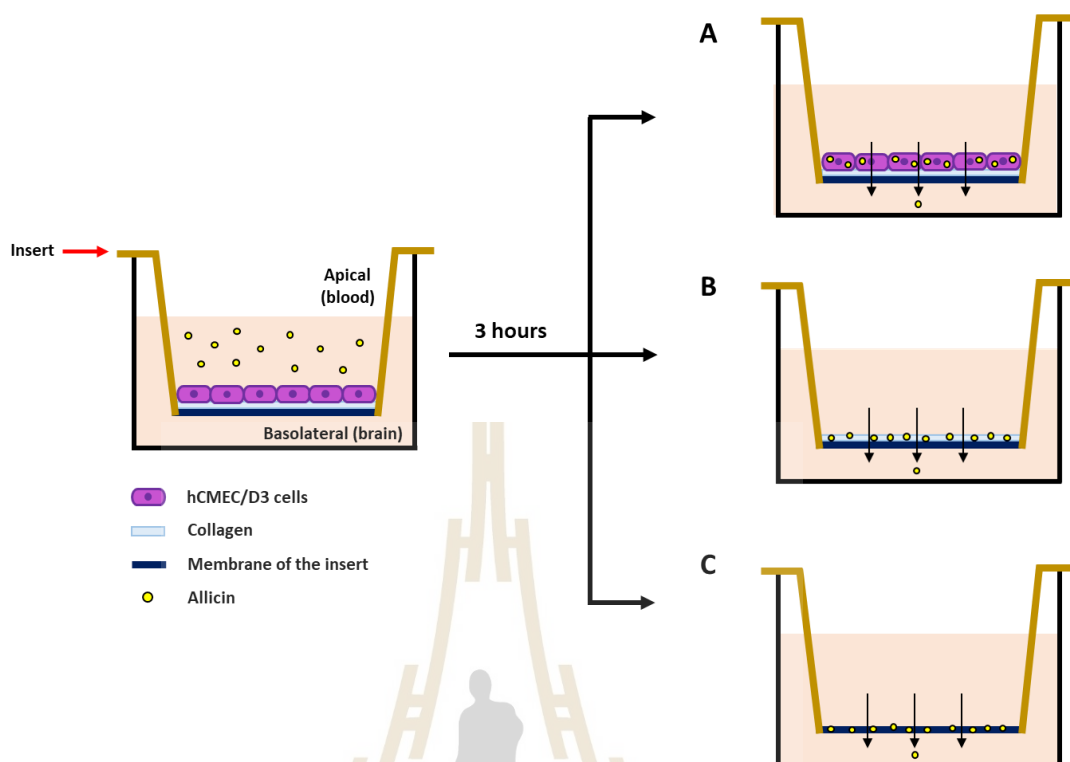


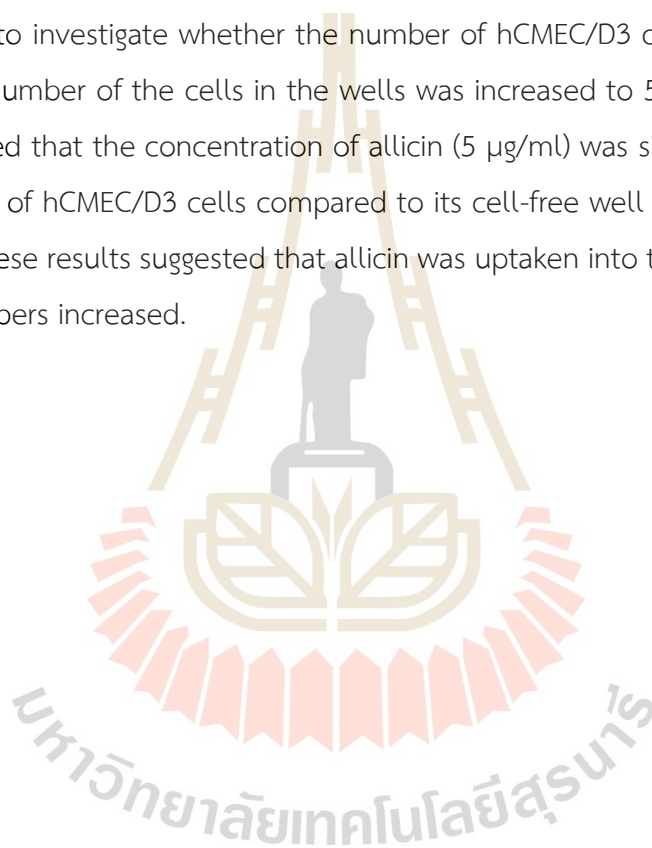
**Figure 4.6** The schematic represents 3 possibilities movement of allicin across the *in vitro* BBB model after 3 h of treatment. (A) Allicin was uptaken into hCMEC/D3 cells. (B) Allicin was trapped in the collagen. (C) Allicin was trapped in the membrane of the insert.

#### 4.4 The uptake of allicin by hCMEC/D3 cells

Cellular uptake experiments were used to indirectly prove the possibility that allicin in the *in vitro* BBB model was uptaken by hCMEC/D3 cells. The non-toxicity concentrations of allicin were used to test hCMEC/D3 cells ( $1 \times 10^4$  cells/well) and their cell-free wells of the 24-well culture plate for 3 h. Then, the concentration of allicin in the supernatant of each well was determined using HPLC analysis. The results showed that the allicin at concentrations of 0.5, 1, and 2  $\mu\text{g/ml}$  were significantly reduced in the presence of hCMEC/D3 cells when compared to its cell-free wells ( $p < 0.05$ ). On the contrary, the concentration of allicin at 5  $\mu\text{g/ml}$  was not statistically different in the presence or absence of hCMEC/D3 cells ( $p > 0.05$ ) (Figure 4.7). Thus,

this finding led to the hypothesis that the cell number of hCMEC/D3 cells used in the experiments might not be sufficient to uptake allicin at 5  $\mu\text{g}/\text{ml}$ . Although the number of the cells used in the *in vitro* BBB model and the cellular uptake experiment were the same, the duration of culturing cells in both assays were different. The cells used in the BBB model were cultured approximately for 21 days; whereas, the cells in the uptake experiments were grown for 1 day. Therefore, the number of the cells that we firstly used was presumably much lower than that in the *in vitro* BBB model.

In order to investigate whether the number of hCMEC/D3 cells affects the allicin uptake, the number of the cells in the wells was increased to  $5 \times 10^4$  cells/well. The results showed that the concentration of allicin (5  $\mu\text{g}/\text{ml}$ ) was significantly reduced in the presence of hCMEC/D3 cells compared to its cell-free well ( $p < 0.05$ ) (Figure 4.8). Therefore, these results suggested that allicin was uptaken into the hCMEC/D3 cells as the cell numbers increased.



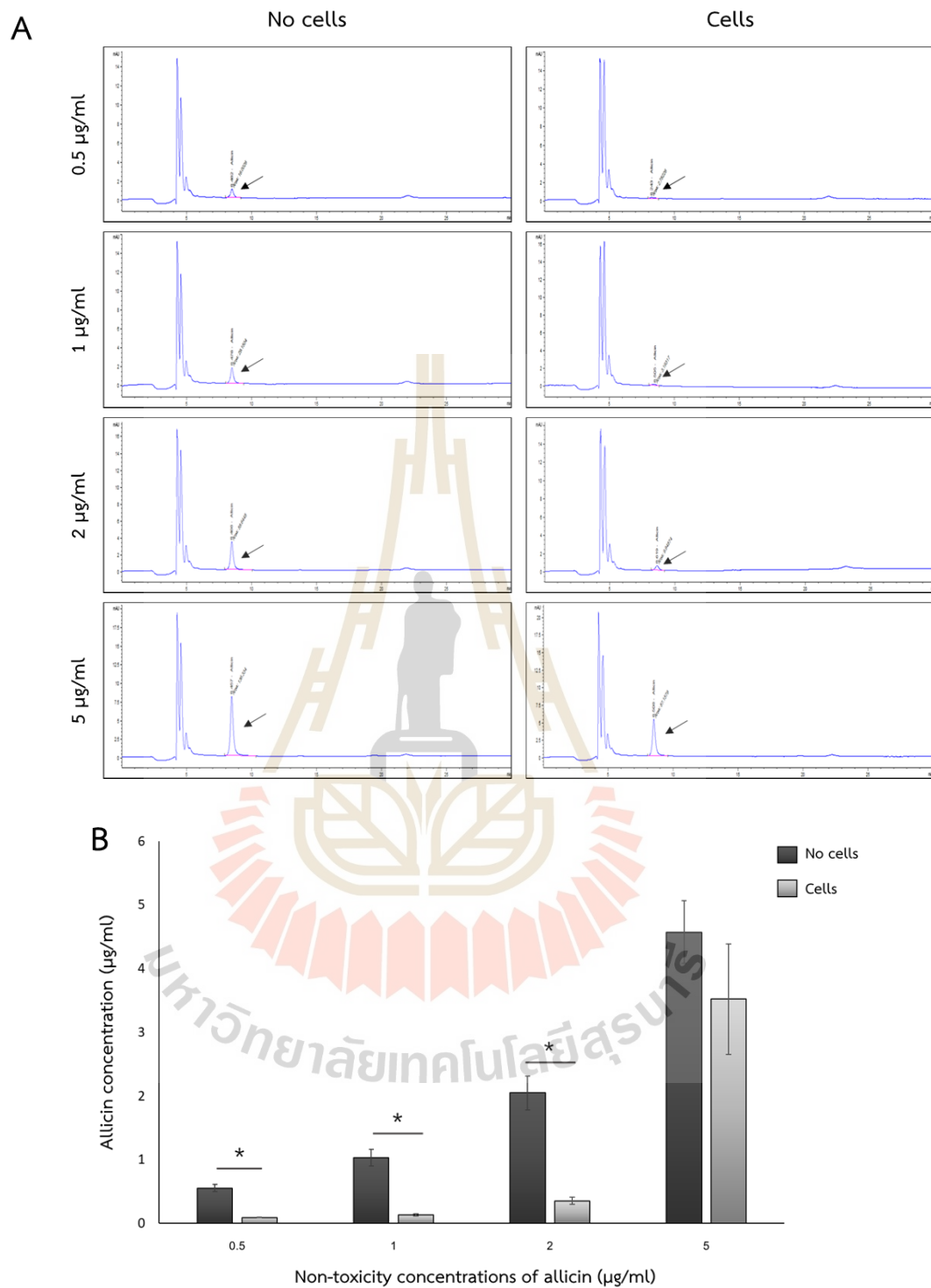


**Figure 4.7** The cellular uptake of alliin by hCMEC/D3 cells. (A) Comparative HPLC chromatograms of alliin between “with cells ( $1 \times 10^4$  cells)” and “without cells” conditions. (B) Quantitative analysis of (A) as alliin concentration in each condition. The values were expressed as mean  $\pm$  SEM ( $n=3$ ). \*  $p < 0.05$ .

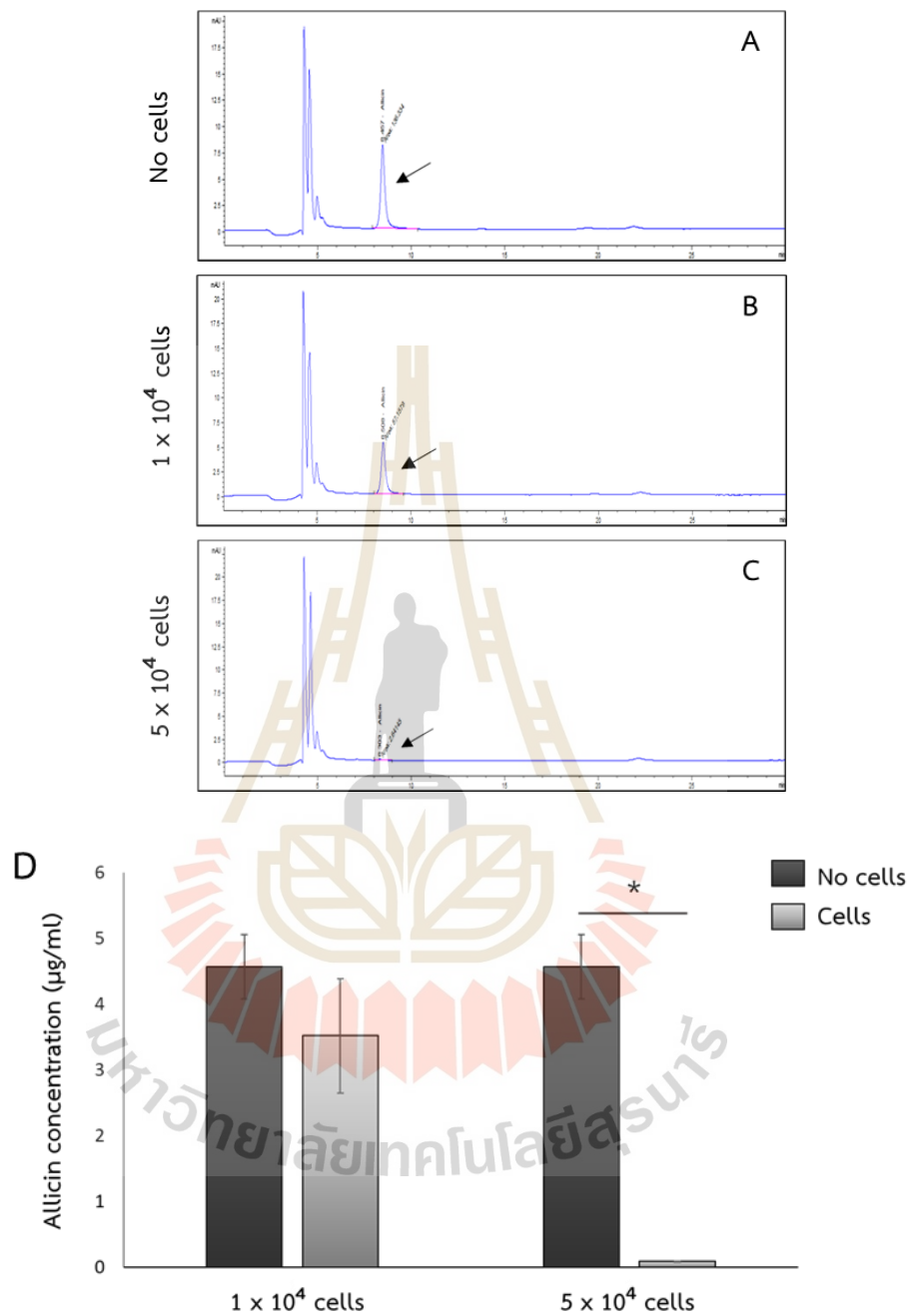


**Figure 4.8** The cellular uptake of alliin (5 µg/ml) by hCMEC/D3 cells. (A-C) Comparative HPLC chromatogram of alliin between “without cells”, “hCMEC/D3 cells (1 x 10<sup>4</sup> cells)”, and “hCMEC/D3 cells (5 x 10<sup>4</sup> cells)” conditions, respectively. (D) Quantitative analysis of (A-C) as alliin concentration in each condition. The values were expressed as mean ± SEM (n=2-3). \*  $p < 0.05$ .

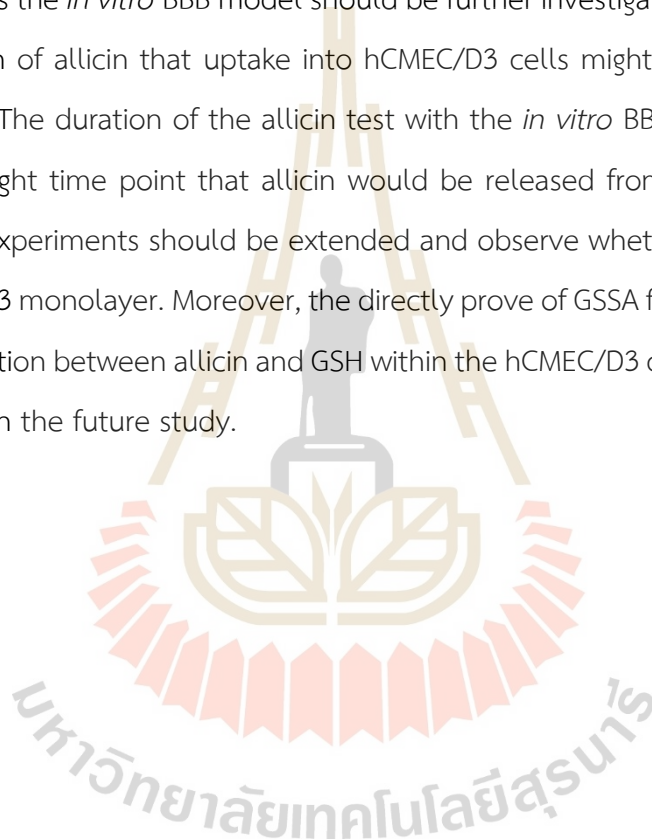
Altogether, the results of the allicin test with the *in vitro* BBB model and the cellular uptake experiments led to the new presumption. These findings suggested that at 3 h of allicin testing, allicin in the AP chamber was absorbed by hCMEC/D3 cells instead of passing to the BL chamber of the *in vitro* BBB model or passing in a small amount, which is unable to be detected by HPLC analysis. According to this presumption, the allicin concentration that was able to cross the *in vitro* BBB model could not be determined in this study.

However, the previous *in vivo* study revealed that allicin has neuroprotective effects on ischemia-reperfusion brain injury (IRBI) (Kong et al., 2017). Moreover, the 2D structure of allicin was predicted to penetrate the BBB by using computer programs (Itepu et al., 2019). Although the present study was not able to conclude that allicin cross BBB, the obtained allicin uptake results were consistent with these findings. Therefore, this study proposes that allicin, a small lipophilic molecule, might be able to pass the BBB via the transcellular route (Figure 2.2 in chapter II). Other small lipid-soluble molecules, which are propranolol, morphine, and midazolam, were also reported to cross the hCMEC/D3 monolayers via the transcellular lipophilic pathway (Poller et al., 2008). According to the effect of allicin on pathogens causing meningitis, the results from this study showed that the MIC of *N. meningitidis* is lower than the highest concentration of the hCMEC/D3 cells uptake. These findings suggested that allicin could potentially affect *N. meningitidis*, the most common and leading cause of bacterial meningitis.

Interestingly, Miron et al. (2000) have investigated the ability of allicin to cross through the phospholipid membrane of artificial phospholipid vesicles loaded with glutathione (GSH) and human red blood cells in which GSH is present. They revealed that allicin can easily penetrate through the phospholipid bilayers to interact with the thiol (SH) groups of GSH and gave the product, S-allylmercaptogluthathione (GSSA), without causing membrane leakage, fusion, or aggregation. These findings also supported that allicin might cross the BBB through the transcellular lipophilic pathway.

However, GSH is a major thiol compound within mammalian cells, including brain endothelial cells (Li et al., 2012). Therefore, their study also provides another clue that the possible reason why the present study could not detect allicin in the BL chamber of the *in vitro* model might be allicin interacts with GSH in hCMEC/D3 cells and already turned into GSSA.

For future studies, the results from the present study suggest that the ability of allicin to cross the *in vitro* BBB model should be further investigated due to the highest concentration of allicin that uptake into hCMEC/D3 cells might have an effect on *N. meningitidis*. The duration of the allicin test with the *in vitro* BBB model at 3 h might not be the right time point that allicin would be released from the cells. Thus, the time of the experiments should be extended and observe whether allicin could cross the hCMEC/D3 monolayer. Moreover, the directly prove of GSSA formation as a product of the interaction between allicin and GSH within the hCMEC/D3 cells should be further investigated in the future study.

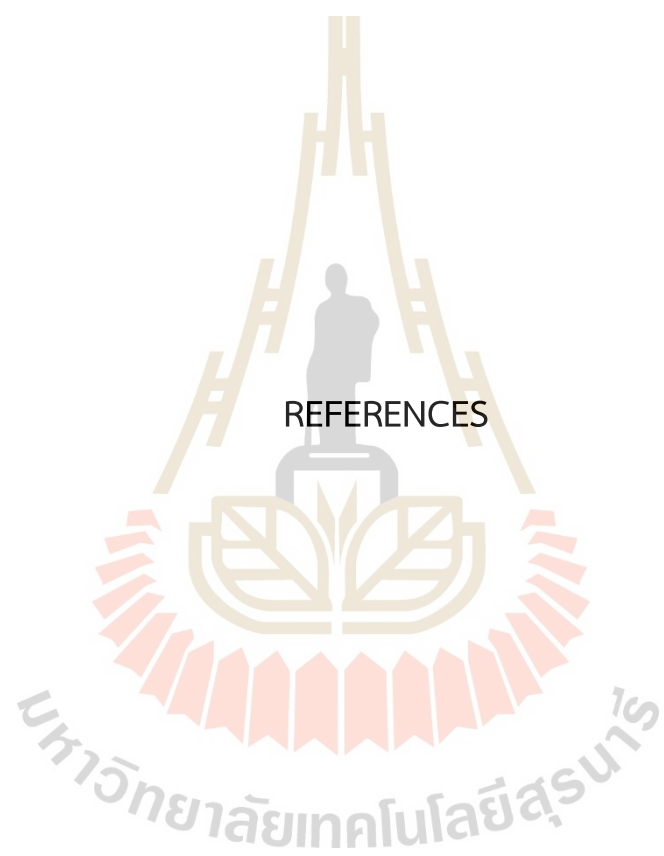


## CHAPTER V

### CONCLUSION

The blood-brain barrier (BBB) plays a crucial role in strictly controlling the passage of substances that circulate within the blood into the central nervous system (CNS). However, the bacterial infections result in dysfunction of BBB, which could lead to meningitis. Bacterial meningitis is a serious disease that requires effective drugs to eliminate the causative pathogens. Allicin, a bioactive compound derived from garlic, has been reported to exhibit antibacterial activity against a wide range of bacteria, including some of the most common meningitis pathogens. In this study, the broth microdilution method demonstrated that *N. meningitidis* was the most sensitive to allicin among the tested pathogens. Moreover, this study is the first to report the MIC value of allicin against the most common meningitis bacteria, *N. meningitidis*. To date, there is no available report regarding the direct evidence that allicin has the ability to pass through BBB. The results of HPLC analysis revealed that allicin could not be detected on both the apical (AP) and basolateral (BL) chambers of the *in vitro* BBB model. However, the HPLC results from the cellular uptake experiments suggested that allicin was uptaken by hCMEC/D3 cells.

In conclusion, the present study could not completely prove that allicin has the ability to cross the *in vitro* BBB model. Nevertheless, the obtained data provide the new presumption that allicin could be uptaken into hCMEC/D3 cells resulting in an undetectable concentration of allicin that passes through the *in vitro* BBB model. Moreover, the results showed that the MIC value of allicin against *N. meningitidis* was lower than the concentration of allicin uptaken in hCMEC/D3 cells, suggesting that allicin could possibly be useful for the treatment of *N. meningitidis*-causing meningitis.



REFERENCES

## REFERENCES

- Abbott, N. J. (2005). Dynamics of CNS barriers: evolution, differentiation, and modulation. *Cellular and Molecular Neurobiology*, 25(1), 5-23.
- Abbott, N. J., Patabendige, A. A., Dolman, D. E., Yusof, S. R., and Begley, D. J. (2010). Structure and function of the blood-brain barrier. *Neurobiology of Disease*, 37(1), 13-25.
- Abramovitz, D., Gavri, S., Harats, D., Levkovitz, H., Mirelman, D., Miron, T., Eldar, M., and Vered, Z. (1999). Allicin-induced decrease in formation of fatty streaks (atherosclerosis) in mice fed a cholesterol-rich diet. *Coronary Artery Disease*, 10, 515-519.
- Agyeman, P., Grandgirard, D., and Leib, S. L. (2017). Neuroinflammation in Bacterial Meningitis. In: Lyck, R., and Enzmann, G. (eds). *The Blood Brain Barrier and Inflammation. Progress in Inflammation Research. Springer*, 213–252.
- Alam, R. T. M., Fawzi, E. M., Alkhalif, M. I., Alansari, W. S., Aleya, L., and Abdel-Daim, M. M. (2018). Anti-inflammatory, immunomodulatory, and antioxidant activities of allicin, norfloxacin, or their combination against *pasteurella multocida* infection in male New Zealand rabbits. *Oxidative Medicine and Cellular Longevity*, 1780956.
- Ankri, S., and Mirelman, D. (1999). Antimicrobial properties of allicin from garlic. *Microbes and Infection*, 1(2), 125-129.
- Bagchi, S., Chhibber, T., Lahooti, B., Verma, A., Borse, V., and Jayant, R. D. (2019). *In-vitro* blood-brain barrier models for drug screening and permeation studies: an overview. *Drug Design, Development and Therapy*, 13, 3591-3605.

- Ballabh, P., Braun, A., and Nedergaard, M. (2004). The blood-brain barrier: an overview: structure, regulation, and clinical implications. *Neurobiology of Disease*, 16(1), 1-13.
- Barar, J., Rafi, M. A., Pourseif, M. M., and Omid, Y. (2016). Blood-brain barrier transport machineries and targeted therapy of brain diseases. *Bioimpacts*, 6(4), 225-248.
- Bicker, J., Alves, G., Fortuna, A., and Falcão, A. (2014). Blood-brain barrier models and their relevance for a successful development of CNS drug delivery systems: a review. *European Journal of Pharmaceutics and Biopharmaceutics*, 87(3), 409-432.
- Bisgard, K. M., Kao, A., Leake, J., Strebel, P. M., Perkins, B. A., and Wharton, M. (1998). *Haemophilus influenzae* invasive disease in the United States, 1994-1995: near disappearance of a vaccine-preventable childhood disease. *Emerging Infectious Diseases*, 4(2), 229-237.
- Booth, R., and Kim, H. (2012). Characterization of a microfluidic *in vitro* model of the blood-brain barrier ( $\mu$ BBB). *Lab on a Chip*, 12(10), 1784-1792.
- Borchorst, S., and Moller, K. (2012). The role of dexamethasone in the treatment of bacterial meningitis - a systematic review. *Acta anaesthesiologica scandinavica*, 56(10), 1210-1221.
- Borlinghaus, J., Albrecht, F., Gruhlke, M. C., Nwachukwu, I. D., and Slusarenko, A. J. (2014). Allicin: chemistry and biological properties. *Molecules*, 19(8), 12591-12618.
- Brouwer, M. C., van de Beek, D., Heckenberg, S. G., Spanjaard, L., and de Gans, J. (2006). Community-acquired *Listeria monocytogenes* meningitis in adults. *Clinical Infectious Diseases*, 43(10), 1233-1238.
- Cavallito, C., and Bailey, J. H. (1944). Allicin, the Antibacterial Principle of *Allium sativum*. I. Isolation, Physical Properties and Antibacterial Action. *Journal of the American Chemical Society*, 66, 1944-1952.

- Cecchelli, R., Dehouck, B., Descamps, L., Fenart, L., Buée-Scherrer, V., Duhem, C., Lundquist, S., Rentfel, M., Torpier, G., and Dehouck, M. P. (1999). *In vitro* model for evaluating drug transport across the blood-brain barrier. *Advanced Drug Delivery Reviews*, 36(2-3), 165-178.
- Chin, E., and Goh, E. (2018). Blood-brain barrier on a chip. *Methods in Cell Biology*, 146, 159-182.
- Curtis, H., Noll, U., Störmann, J., and Slusarenko, A. J. (2004). Broad-spectrum activity of the volatile phytoanticipin allicin in extracts of garlic (*Allium sativum* L.) against plant pathogenic bacteria, fungi and Oomycetes. *Physiological and Molecular Plant Pathology*, 65, 79-89.
- Cutler, R. R., and Wilson, P. (2004). Antibacterial activity of a new, stable, aqueous extract of allicin against methicillin-resistant *Staphylococcus aureus*, *British Journal of Biomedical Science*, 61(2), 71-74.
- Daneman, R., and Prat, A. (2015). The blood-brain barrier. *Cold Spring Harbor Perspectives in Biology*, 7(1).
- Dehouck, M. P., Méresse, S., Delorme, P., Fruchart, J. C., and Cecchelli, R. (1990). An easier, reproducible, and mass-production method to study the blood-brain barrier *in vitro*. *Journal of Neurochemistry*, 54(5), 1798-1801.
- Deli, M. A., Abrahám, C. S., Kataoka, Y., and Niwa, M. (2005). Permeability studies on *in vitro* blood-brain barrier models: physiology, pathology, and pharmacology. *Cellular and Molecular Neurobiology*, 25(1), 59-127.
- Daniels, B. P., Cruz-Orengo, L., Pasiaka, T. J., Couraud, P., Romero, I. A., Weksler, B., Cooper, J. A., Doering, T. L., and Klein, R. S. (2013). Immortalized human cerebral microvascular endothelial cells maintain the properties of primary cells in an *in vitro* model of immune migration across the blood brain barrier. *Journal of Neuroscience Methods*, 212(1), 173-179.

- Doran, K. S., Fulde, M., Gratz, N., Kim, B. J., Nau, R., Prasadarao, N., Schubert-Unkmeir, A., Tuomanen, E. I., and Valentin-Weigand, P. (2016). Host-pathogen interactions in bacterial meningitis. *Acta Neuropathologica*, 131(2), 185-209.
- Edmond, K., Clark, A., Korczak, V. S., Sanderson, C., Griffiths, U. K., and Rudan, I. (2010). Global and regional risk of disabling sequelae from bacterial meningitis: a systematic review and meta-analysis. *The Lancet Infectious Diseases*, 10(5), 317-328.
- Ekizoğlu, M. (2017). Infectious Diseases of the Brain. In *Nanotechnology Methods for Neurological Diseases and Brain Tumors*. Elsevier, 291-315.
- Ellmore, G. S., and Feldberg, R. S. (1994). Allin Lyase Localization in Bundle Sheaths of the Garlic Clove (*Allium sativum*). *American Journal of Botany*, 81, 89-94.
- Feldberg, R. S., Chang, S. C., Kotik, A. N., Nadler, M., Neuwirth, Z., Sundstrom, D. C., and Thompson, N. H. (1988). *In vitro* mechanism of inhibition of bacterial cell growth by allicin. *Antimicrobial Agents and Chemotherapy*, 32, 1763-1768.
- Focke, M., Feld, A., and Lichtenthaler, H. K. (1990). Allicin, a naturally occurring antibiotic from garlic, specifically inhibits acetyl-CoA synthetase. *FEBS Letters*, 261, 106-108.
- Grieb, P., Forster, R. E., Strome, D., Goodwin, C. W., and Pape, P. C. (1985). O<sub>2</sub> exchange between blood and brain tissues studied with <sup>18</sup>O<sub>2</sub> indicator-dilution technique. *Journal of Applied Physiology*, 58, 1929-1941.
- Gupta, K. C., and Viswanathan, R. (1955). Combined action of streptomycin and chloramphenicol with plant antibiotics against tubercle bacilli. I. Streptomycin and chloramphenicol with cepharanthine. II. Streptomycin and allicin. *Antibiotics & chemotherapy*, 5(1), 24-27.
- Helms, H. C., Abbott, N. J., Burek, M., Cecchelli, R., Couraud, P. O., Deli, M. A., Forster, C., Galla, H. J., Romeo, I. A., Shusta, E. V., Stebbins, M. J., Vandenhoute, E., Weskler, B., and Brodin, B. (2016). *In vitro* models of the blood-brain barrier: An overview of commonly used brain endothelial cell culture models and

- guidelines for their use. *Journal of Cerebral Blood Flow & Metabolism*, 36(5), 862-890.
- Himanshu, R., Jakir, P., Pradnya, H., Suneel, P., and Ramesh, S. (2013). The impact of permeability enhancers on assessment for monolayer of colon adenocarcinoma cell line (CACO-2) used in *in vitro* permeability assay. *Journal of Drug Delivery & Therapeutics*, 3(3), 20-29.
- Hirsch, K., Danilenko, M., Giat, J., Miron, T., Rabinkov, A., Wilchek, M., and Sharoni, Y. (2000). Effect of purified allicin, the major ingredient of freshly crushed garlic, on cancer cell proliferation. *Nutrition and Cancer*, 38(2), 245-254.
- Hitchcock, S. A., and Pennington, L. D. (2006). Structure-brain exposure relationships. *Journal of medicinal chemistry*, 49(26), 7559-7583.
- Hoffman, O., and Weber, R. J. (2009). Pathophysiology and treatment of bacterial meningitis. *Therapeutic Advances in Neurological Disorders*, 2(6), 1-7.
- Hunter, R., Cairn, M., and Stellenboom, N. (2005). Thiolsulfinate allicin from garlic: inspiration for a new antimicrobial agent. *Annals of the New York Academy of Sciences*, 1056, 234-241.
- Ilic, D., Nikolic, V., Nikolic, L., Stankovic, M., Stanojevic, L., and Cakic, M. (2011). Allicin and related compounds: Biosynthesis, synthesis and pharmacological activity. *Facta Universitatis, Series: Physics, Chemistry and Technology*, 9(1), 9-20.
- Imani Rad, H., Arzanlou, M., Ranjbar Omid, M., Ravaji, S., and Peeri Doghaheh, H. (2017). Effect of culture media on chemical stability and antibacterial activity of allicin. *Journal of functional foods*, 28, 321-325.
- Itepu, V. E., Umezina, O. J., Ilukho, F. A., Collins, D. A., and Cosmas, S. (2019). The effect of structural modification on the blood brain barrier permeation properties of allicin. *Asian Journal of Research in Biochemistry*, 1-7.
- Jackson, S., Meeks, C., Vezina, A., Robey, R. W., Tanner, K., and Gottesman, M. M. (2019). Model systems for studying the blood-brain barrier: Applications and challenges. *Biomaterials*, 214, 119217.

- Jena, L., McErlean, E., and McCarthy, H. (2020). Delivery across the blood-brain barrier: nanomedicine for glioblastoma multiforme. *Drug Delivery and Translational Research*, 10(2), 304-318.
- Jeong, J. Y., Kwon, H. B., Ahn, J. C., Kang, D., Kwon, S. H., Park, J. A., and Kim, K. W. (2008). Functional and developmental analysis of the blood-brain barrier in zebrafish. *Brain Research Bulletin*, 75(5), 619-628.
- Khodavandi, A., Alizadeh, F., Harmal, N. S., Sidik, S. M., Othman, F., Sekawi, Z., Jahromi, M. A. F., Ng, K. P., and Chong, P. P. (2011). Comparison between efficacy of allicin and fluconazole against *Candida albicans* *in vitro* and in a systemic candidiasis mouse model. *FEMS Microbiology Letters*, 315(2), 87-93.
- Kim, K. (2003). Pathogenesis of bacterial meningitis: from bacteraemia to neuronal injury. *Nature Reviews Neuroscience*, 4(5), 376-385.
- Kim, K. (2008). Mechanisms of microbial traversal of the blood-brain barrier. *Nature Reviews Microbiology*, 6(8), 625-634.
- Kong, X., Gong, S., Su, L., Li, C., and Kong, Y. (2017). Neuroprotective effects of allicin on ischemia-reperfusion brain injury. *Oncotarget*, 8, 104492-104507.
- Larsen J. M., Martin D. R., and Byrne M. E. (2014). Recent advances in delivery through the blood-brain barrier. *Current Topics in Medicinal Chemistry*, 14, 1148-1160.
- Li, C., Jing, H., Ma, G., and Liang, P. (2018). Allicin induces apoptosis through activation of both intrinsic and extrinsic pathways in glioma cells. *Molecular Medicine Reports*, 17(4), 5976-5981.
- Li, W., Busu, C., Circu, M. L., and Aw, T. (2012). Glutathione in cerebral microvascular endothelial biology and pathobiology: implications for brain homeostasis. *International Journal of Cell Biology*, 2012, 434971.
- Lippmann, E. S., Al-Ahmad, A., Palecek, S. P., and Shusta, E. V. (2013). Modeling the blood-brain barrier using stem cell sources. *Fluids and Barriers of the CNS*, 10(1), 2.

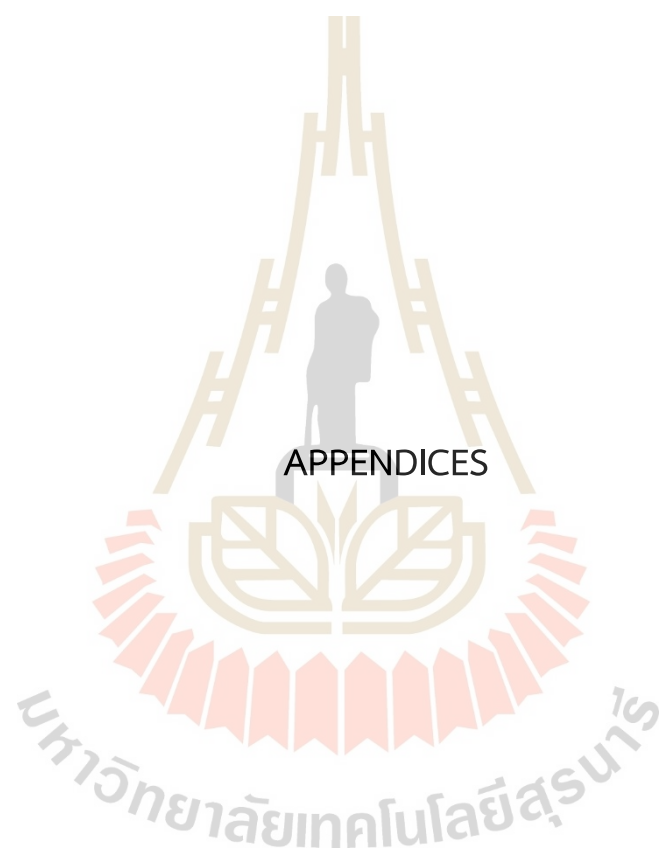
- Lu, C., Zhao, Y., Wong, H., Cai, J., Peng, L., and Tian, X. (2014). Current approaches to enhance CNS delivery of drugs across the brain barriers. *International Journal of Nanomedicine*, 9, 2241-2257.
- MacNeil, J. R., Blain, A. E., Wang, X., and Cohn, A. C. (2018). Current Epidemiology and Trends in Meningococcal Disease-United States, 1996-2015. *Clinical Infectious Diseases*, 66(8), 1276-1281.
- Malina, K., Cooper, I., and Teichberg, V. (2009). Closing the gap between the *in-vivo* and *in-vitro* blood-brain barrier tightness. *Brain Research*, 1284, 12-21.
- Mirelman, D., Monheit, D., and Varon S. (1987). Inhibition of growth of *Entamoeba histolytica* by allicin, the active principle of garlic extract (*Allium sativum*). *The Journal of Infectious Diseases*, 156(1), 243-244.
- Mösbauer, K., Fritsch, V. N., Adrian, L., Bernhardt, J., Gruhlke, M. C. H., Slusarenko, A. J., Niemeyer, D., and Antelmann, H. (2021). The effect of allicin on the proteome of SARS-CoV-2 Infected Calu-3 cells. *Frontiers in Microbiology*, 12, 746795.
- Nakagawa, S., Deli, M. A., Kawaguchi, H., Shimizudani, T., Shimono, T., Kittel, A., Tanaka, K., Niwa, M. (2009). A new blood-brain barrier model using primary rat brain endothelial cells, pericytes and astrocytes. *Neurochemistry International*, 54(3-4), 253-263.
- Neuhaus, W., Lauer, R., Oelzant, S., Fringeli, U. P., Ecker, G. F., and Noe, C.R. (2006). A novel flow based hollow-fiber blood-brain barrier *in vitro* model with immortalised cell line PBMEC/C1-2. *Journal of Biotechnology*, 125(1), 127-141.
- Nkabinde, L. A., Shoba-Zikhali, L. N. N., Semete-Makokotlela, B., Kalombo, L., Swai, H. S., Hayeshi, R., Naicker, B., Hillie, T. K., and Hamman, J. H. (2012). Permeation of PLGA nanoparticles across different *in vitro* models. *Current Drug Delivery*, 9(6), 617-627.
- Oommen, S., Anto, R. J., Srinivas, G., and Karunakaran, D. (2004). Allicin (from garlic) induces caspase-mediated apoptosis in cancer cells. *European journal of pharmacology*, 485(1-3), 97-103.

- Ossama, M., Hathout, R. M., Attia, D. A., and Mortada, N. D. (2019). Enhanced Allicin Cytotoxicity on HEPG-2 Cells Using Glycyrrhetic Acid Surface-Decorated Gelatin Nanoparticles. *ACS Omega*, 4(6), 11293-11300
- Ozolin, O. N., Uteshev, T. A., Kim, I. A., Deev, A. A., and Kamzolova, S. G. (1990). Specific modification of the alpha-subunit of Escherichia coli RNAS polymerase by monomeric derivative of fluorescein mercuric acetate. *Molekuliarnaia Biologiia (Moskva)*, 24, 1057-1066.
- Pandey, P. K., Sharma, A. K., and Gupta, U. (2015). Blood brain barrier: An overview on strategies in drug delivery, realistic *in vitro* modeling and *in vivo* live tracking. *Tissue Barriers*, 4(1).
- Pardridge, W. M., Eisenberg, J., and Yang, J. (1985). Human blood– brain barrier insulin receptor. *Journal of Neurochemistry*, 44, 1771-1778.
- Pardridge, W. M., Triguero, D., Yang, J., and Cancilla, P. A. (1990). Comparison of *in vitro* and *in vivo* models of drug transcytosis through the blood-brain barrier. *The Journal of Pharmacology and Experimental Therapeutics*, 253(2), 884-891.
- Passeleu-Le Bourdonnec, C., Carrupt, P., Scherrmann, J. M., and Martel, S. (2013). Methodologies to assess drug permeation through the blood-brain barrier for pharmaceutical research. *Pharmaceutical Research*, 30(11), 2729-2756.
- Pintado, V., Pazos, R., Jiménez-Mejías, M. E., Rodríguez-Guardado, A., Gil, A., García-Lechuz, J. M., Cabellos, C., Chaves, F., Domingo, P., Ramos, A., Pérez-Cecilia, E., and Domingo, D. (2012). Methicillin-resistant *Staphylococcus aureus* meningitis in adults. *Medicine*, 91, 10-17.
- Poller, B., Gutmann, H., Krähenbühl, S., Weksler, B., Romero, I., Couraud, P. O., Tuffin, G., Drewe, J., and Huwyler, J. (2008). The human brain endothelial cell line hCMEC/D3 as a human blood-brain barrier model for drug transport studies. *Journal of Neurochemistry*, 107(5), 1358-1368.
- Reiter, J., Levina, N., van der Linden, M., Gruhlke, M., Martin, C., and Slusarenko, A. J. (2017). Diallylthiosulfinate (Allicin), a volatile antimicrobial from garlic (*Allium*

- sativum*), kills human lung pathogenic bacteria, including MDR strains, as a vapor. *Molecules*, 22(10).
- Ried, K., Frank, O. R., Stocks, N. P., Fakler, P., and Sullivan, T. (2008). Effect of garlic on blood pressure: a systematic review and meta-analysis. *BMC Cardiovascular Disorders*, 8, 13.
- Rouphael, N. G., and Stephens, D. S. (2012). *Neisseria meningitidis*: biology, microbiology, and epidemiology. *Methods in Molecular Biology*, 799, 1-20.
- Shadkchan, Y., Shemesh, E., Mirelman, D., Miron, T., Rabinkov, A., Wilchek, M., and Osherov, N. (2004). Efficacy of allicin, the reactive molecule of garlic, in inhibiting *Aspergillus* spp. in vitro, and in a murine model of disseminated aspergillosis. *Journal of Antimicrobial Chemotherapy*, 53(5), 832-836.
- Sharma, B., Luhach, K., and Kulkarni, G. T. (2019). *In vitro* and *in vivo* models of BBB to evaluate brain targeting drug delivery. *Brain Targeted Drug Delivery System*, 53-101.
- Shrivastava, A., and Garg, H. K. (2015). Allicin as a dermal antibiotic against infections. *World journal of pharmaceutical research*, 4(12), 1052-1056.
- Sivandzade, F., and Cucullo, L. (2018). *In-vitro* blood-brain barrier modeling: A review of modern and fast-advancing technologies. *Journal of Cerebral Blood Flow & Metabolism*, 38(10), 1667-1681.
- Sobue, K., Yamamoto, N., Yoneda, K., Hodgson, M. E., Yamashiro, K., Tsuruoka, N., Tsuda, T., Katsuya, H., Miura, Y., Asai, K., and Kato, T. (1999). Induction of blood-brain barrier properties in immortalized bovine brain endothelial cells by astrocytic factors. *Journal of Neuroscience Research*, 35(2), 155-164.
- Stephens, D. S. (2007). Conquering the Meningococcus. *FEMS Microbiology Reviews*, 31(1), 3-14.
- Tanongkankit, Y., Kalantakuwan, S., Varith, J., and Narkprasom, K. (2019). Ultrasonic-assisted extraction of allicin and its stability during storage. *Food and Applied Bioscience Journal*, 7(2), 17-31.

- Tóth, A., Veszélka, V., Nakagawa, S., Niwa, M., and Deli, M. A. (2011). Patented *in vitro* blood-brain barrier models in CNS drug discovery. *Recent Patents on CNS Drug Discovery*, 6(2), 107-118.
- Tunkel, A. R., Hartman, B. J., Kaplan, S. L., Kaufman, B. A., Roos, K. L., Scheld, W. M., and Whitley, R. J. (2004). Practice guidelines for the management of bacterial meningitis. *Clinical Infectious Diseases*, 39(9), 1267-1284.
- Tzeng, Y., and Stephens, D. S. (2000). Epidemiology and pathogenesis of *Neisseria meningitidis*. *Microbes and Infection*, 2(6), 687-700.
- Umans, R. A., and Taylor, M. R. (2012). Zebrafish as a model to study drug transporters at the blood-brain barrier. *Clinical Pharmacology & Therapeutics*, 92(5), 567-570.
- Van de Beek, D., de Gans, J., Tunkel, A. R., and Wijdicks, E. F. (2006). Community-acquired bacterial meningitis in adults. *The New England Journal of Medicine*, 354(1), 44-53.
- Wang, H., Li, X., Liu, X., Shen, D., Qiu, Y., Zhang, X., and Song, J. (2014). Influence of pH, concentration and light on stability of allicin in garlic (*Allium sativum* L.) aqueous extract as measured by UPLC. *Journal of the Science of Food and Agriculture*, 95(9), 1838-1844.
- Weber, N. D., Anderson, D. O., North, J. A., Murray, B. K., Lawson, L. D., and Hughes, B. G. (1992). *In vitro* virucidal effects of *Allium sativum* (garlic) extract and compounds. *Planta Medica*, 58, 417-423.
- Weisfelt, M., van de Beek, D., Spanjaard, L., Reitsma, J. B., and de Gans, J. (2006). Clinical features, complications, and outcome in adults with pneumococcal meningitis: a prospective case series. *The Lancet Neurology*, 5(2), 123-129.
- Weksler, B. B., Subileau, E. A., Perrière, N., Charneau, P., Holloway, K., Leveque, M., Tricoire-Leignel, H., Nicotra, A., Bourdoulous, S., Turowski, P., Male, D. K., Roux, F., Greenwood, J., Romero, I. A., and Couraud, P. O. (2005). Blood-brain barrier-

- specific properties of a human adult brain endothelial cell line. *The FASEB Journal*, 19(13), 1872-1874.
- Weksler, B. B., Romero, I. A., and Couraud, P. O. (2013). The hCMEC/D3 cell line as a model of the human blood brain barrier. *Fluids and Barriers of the CNS*, 10(1), 16.
- Weeranantanapan, O., Satsantitham, K., Sritangos, P., and Chudapongse, N. (2020). Allicin suppresses human glioblastoma cell growth by inducing cell cycle arrest and apoptosis, and by promoting autophagy. *Archives of Biological Sciences*, 72(3), 313-319.
- Wilhelm, I., Fazakas, C., and Krizbai, I. A. (2011). *In vitro* models of the blood-brain barrier. *Acta Neurobiologiae Experimentalis*, 71(1), 113-128.
- Wolff, A., Antfolk, M., Brodin, B., and Tenje, M. (2015). *In vitro* blood-brain barrier models-an overview of established models and new microfluidic approaches. *Journal of pharmaceutical sciences*, 104(9), 2727-2746.
- Zhang, Y., and Pardridge, W. M. (2001). Rapid transferrin efflux from brain to blood across the blood – brain barrier. *Journal of Neurochemistry*, 76, 1597-1600.



## APPENDIX A

### LABORATORY EQUIPMENT

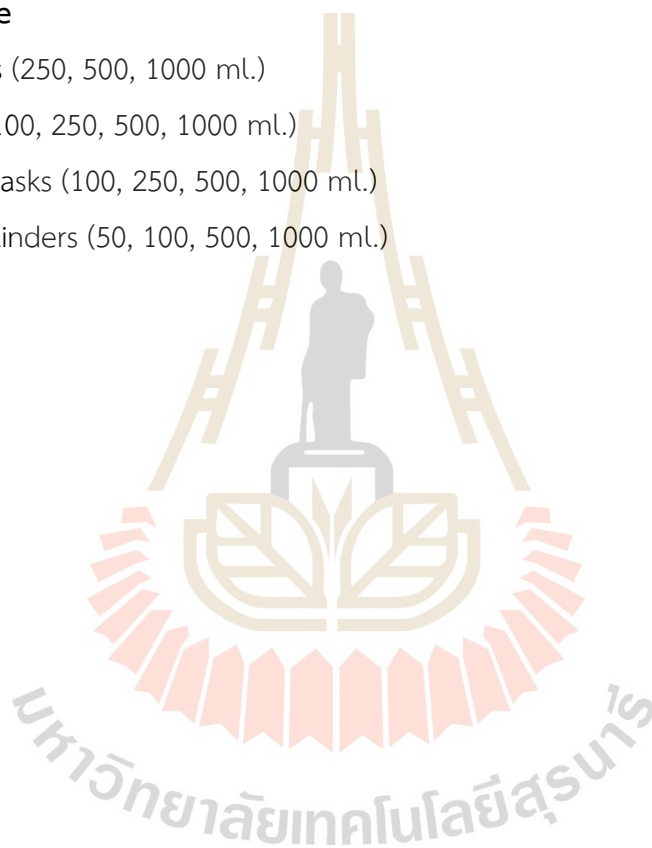
#### A.1 Equipment

Name	Source
Autoclave	Tomy Kogyo, Japan
HPLC 1260	Agilent, USA
Hot air oven	Mettler, Germany
Vortex mixer	Finecpr, Korea
Laminar flow	Esco, Singapore
Haemocytometer	Boeco, Germany
Electronic balance	Shimadzu, Japan
Centrifuge CT15RT	Techcomp, Hong Kong
Microscope CKX41SF	Olympus, Philippines
Hotplate magnetic stirrer	Merck, USA
Epithelial Volt-Ohm meter	Millipore, USA
Incubator shaker Innova 42R	Eppendorf, Germany
T80+ UV/VIS spectrophotometer	PG Instruments, UK
Forma Series II water-jacketed CO <sub>2</sub> Incubator	Thermo scientific, USA
Multiskan Go microplate spectrophotometer	Thermo scientific, Finland
Varioskan Lux multimode microplate reader	Thermo scientific, Singapore
Autopipette (1-10, 2-20, 20-200, 100-1000 µl.)	Gilson, France
Cuvettes	VWR, Germany
Petri dish	Biologix, China
Cryovial (1.8 ml.)	SPL life science, Korea
Microtubes (0.6 ml.)	Axygen, China
Conical tube (15, 50 ml.)	Corning, China
24-well cell culture plate	Corning, USA

96-well cell culture plate	Corning, China
Cell culture flask (75 cm <sup>2</sup> .)	Nunc, China
Sterile syringe filter (0.2 µm.)	Corning, Germany
Microcentrifuge tube (1.5 ml.)	Hycon, Thailand
Syringe without needle (3 ml.)	Nipro, Thailand
24-well hanging inserts (0.4 µm PET)	Millicell, Germany
Pipette tips (0.5-10, 1-200, 100-1000 µl.)	Kirgen, China

### A.2 Glassware

Duran bottles (250, 500, 1000 ml.)
Beakers (50, 100, 250, 500, 1000 ml.)
Erlenmeyer flasks (100, 250, 500, 1000 ml.)
Measuring cylinders (50, 100, 500, 1000 ml.)



APPENDIX B  
STANDARD CURVE OF ALLICIN

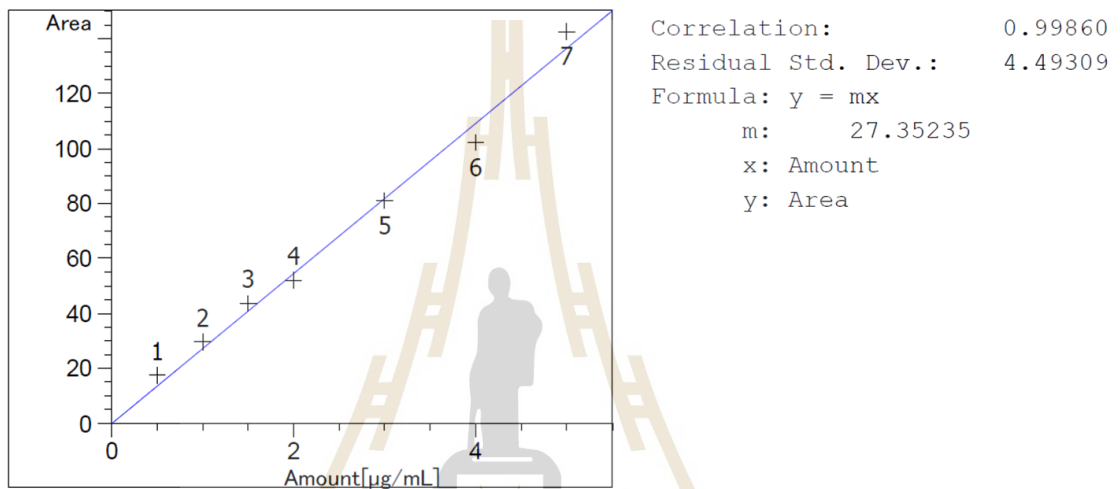


**Figure B** The standard curve of allucin was established by the peak area of allucin at concentrations of 0.5, 1, 1.5, 2, 3, 4, and 5 µg/ml.

## APPENDIX C

### TEMPERATURE TEST OF ALLICIN

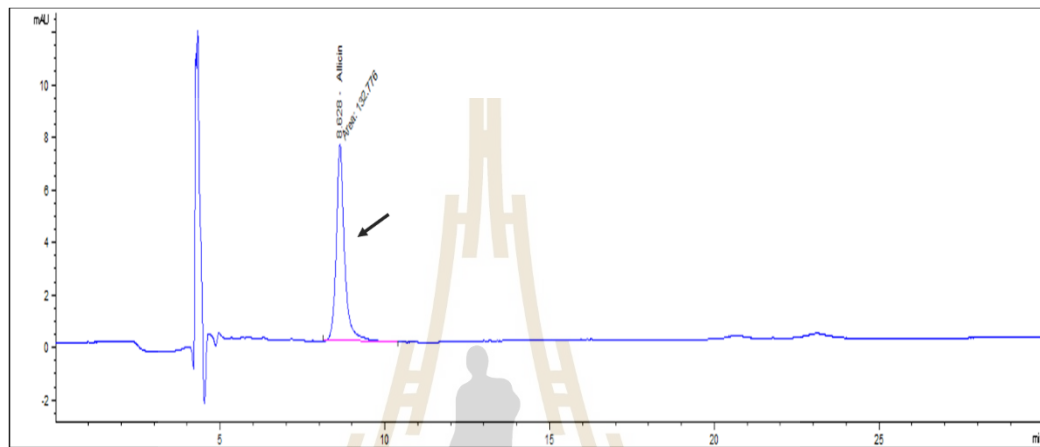


**Figure C** HPLC chromatogram of alllicin sample from the opened cap eppendorf containing alllicin 5 µg/ml and incubated at 37°C for 3 h.

**Table C** Alllicin concentration of the sample from the temperature test.

Sample	Alllicin concentration (µg/ml)
Alllicin sample from the opened cap eppendorf containing alllicin 5 µg/ml and incubated at 37°C for 3 h	4.91 ± 0.7

The value was expressed as mean ± SEM (n=3).

## CURRICULUM VITAE

**Name:** Miss Kankawi Satsantitham

**Date of birth:** March 21, 1996

**Place of birth:** Nakhon Ratchasima, Thailand

**Education:**

2015-2019 Bachelor of Science (Biology), Institute of Science, Suranaree University of Technology, Nakhon Ratchasima, Thailand

2019-Present Master of Science student (Microbiology), School of Preclinical Sciences, Institute of Science, Suranaree University of Technology, Nakhon Ratchasima, Thailand

**Publication:**

O. Weeranantanapan, K. Satsantitham, P. Sritangos, and N. Chudapongse, "Allicin suppresses human glioblastoma cell growth by inducing cell cycle arrest and apoptosis, and by promoting autophagy," Arch Biol Sci, 73, 313-319 (2020).

**Grant:** One Research One Grant (OROG) scholarship, 2019-2021.